Direct major- and trace-element analyses of rock varnish by high resolution laser ablation inductively-coupled plasma mass spectrometry (LA-ICPMS)

David M. Wayne [a,*], Tammy A. Diaz [b,1], Robert J. Fairhurst [b], Richard L. Orndorff [c], Douglas V. Pete [d]

[a] *Nuclear Materials Technology Division, NMT-15, MS-E530, Los Alamos National Laboratory, Los Alamos, NM 87545, United States*
[b] *Department of Geoscience, University of Nevada, Las Vegas NV 89154-4010, United States*
[c] *Department of Geology, Eastern Washington University, Cheney, WA 99004-2439, United States*
[d] *Nuclear Materials Technology Division, NMT-16, MS G-721, Los Alamos National Laboratory, Los Alamos, NM 87545, United States*

Abstract

Laser ablation inductively coupled plasma mass spectrometry (LA-ICPMS) was used to determine major and trace element concentrations in rock varnish samples from the Lahontan Range, near Fallon, NV and from a remote wilderness area near the San Juan River, in southeastern Utah. The data indicate that rapid LA-ICPMS analyses provide ample analytical resolution for semi-quantitative compositional determinations of both trace and major elements in the varnish despite the presence of a rock substrate component in most analyses. The overall major element contents of rock varnish from the two localities are grossly similar to rock varnish from other locations analyzed by solution ICPMS, electron microprobe, and energy dispersive scanning electron microscopy (SEM). Differences between microprobe and LA-ICPMS analyses may stem from different sampling scales and different degrees of substrate involvement. It was possible to detect significant variations in trace element contents in the rock varnish samples. The Lahontan Range is situated within a belt of W mineralization, and varnish from that locality contained significantly higher W and Mo contents than varnish from localities outside the W belt. Lead, Tl, Bi, Cd and As contents of varnish-coated pebbles from near the San Juan River in southeastern Utah, varied by an order of magnitude as a function of the position of the sampling site on the pebble. Elevated heavy element contents on the skyward-facing varnish surfaces indicate that heavy elements may be preferentially scavenged at the locations most likely to receive direct inputs of atmospherically-deposited airborne particulates. The source of metal-rich airborne particulates, in this case, is probably any one of several large coal-fired power plants in the Four Corners region, proximal to the San Juan study area. These patterns indicate that rock varnish chemistry is influenced by atmospherically-derived fluxes of both dissolved and particulate constituents, and that rock varnish can be used as a passive environmental indicator for a wide variety of elements, in much the same manner as moss and lichens.
© 2006 Elsevier Ltd. All rights reserved.

---

* Corresponding author. Tel.: +1 505 665 7552; fax: +1 505 665 5982.
  E-mail address: d-wayne@lanl.gov (D.M. Wayne).
  [1] Present address: New Mexico Environment Department, Hazardous Waste Bureau, 2905 Rodeo Park Drive East, Building 1, Santa Fe, NM, 87505, USA.

1. Introduction

Rock varnish, also known as desert varnish, is a naturally-occurring, highly indurated, dark brown rock coating composed of clay minerals and Mn–Fe oxyhydroxides. It occurs most frequently in semi-arid and arid climes, on all rock types (Perry and Adams, 1978), including meteorites (Lee and Bland, 2003). Varnish thickness may vary from ∼5 to over 200 μm on a single surface (Diaz, 2004), and is greatest in minute depressions and pits in rock surfaces (Liu and Broecker, 2000; Broecker and Liu, 2001). Outer layers are subject to abrasion and exfoliation in arid, windy environments (Reneau, 1993). Cross-sections show that rock varnish is compositionally stratified into layers containing differing percentages of clays and detrital particulate material versus chemically-deposited Fe and Mn oxyhydroxides (Potter and Rossman, 1977; Perry and Adams, 1978; Raymond et al., 1991; Reneau et al., 1992; Krinsley, 1998; Liu et al., 2000; Broecker and Liu, 2001). The proportions of these components can vary laterally and vertically on a millimeter- to sub-millimeter scale (Reneau, 1993).

The origin of rock varnish is external to the rock surfaces it coats (Engel and Sharp, 1958; Potter and Rossman, 1977; Perry and Adams, 1978; Dorn and Oberlander, 1982; Broecker and Liu, 2001). Though Fe- and Mn-rich coatings may be deposited on rock surfaces by direct precipitation from running water, the role of biogenic processes in rock varnish formation has long been suspected (Hunt, 1961; Bauman, 1976; Perry and Adams, 1978; Krumbein and Jens, 1981; Taylor-George et al., 1983). In arid environments, much of the textural evidence for microbially mediated rock varnish formation is probably obliterated by wind erosion, diagenetic effects, and surface weathering. However, recent scanning- and transmission electron microscope (SEM, TEM) studies indicate that rock varnish contains bacterial and fungal trace fossils (Krinsley, 1998; Bargar et al., 2000; Probst et al., 2002; Flood et al., 2003). Recent direct observations of Mn- and Fe-oxidizing microbial communities (Spilde et al., 2002), bacterial amino acids, enzymes and metabolites (Nagy et al., 1991; Edwards et al., 2004; Perry and Kolb, 2004; Kolb et al., 2004), and bacterial RNA and DNA (Eppard et al., 1996; Spilde et al., 2002; Perry et al., 2002; Diaz, 2004; Perry and Kolb, 2004; Kolb et al., 2004; Kuhlman et al., 2005) in and on rock varnish, and ferromanganiferous varnish-like coat-ings, support the contention that rock varnish formation is somehow assisted or catalyzed by the metabolic processes of Mn-oxidizing bacteria, or fungi.

The most abundant Fe- and Mn-oxyhydroxide phases in rock varnish are goethite, birnessite, and todorokite (McKeown and Post, 2001). These minerals are known to adsorb a wide range of elements directly from oceanic and fresh surface waters, and exert considerable control on the chemistry and distribution of heavy metals in soils (Post, 1999; Ferris et al., 2000; Palumbo et al., 2000, 2001; Manceau et al., 2003; Nelson and Lion, 2003; Tebo et al., 2004). Birnessite also scavenges actinides directly from solution (Post, 1999; Dyer et al., 2000; Al-Attar and Dyer, 2002; Misaelides et al., 2002). Though the ferromanganiferous phases are chemical precipitates, most of the clays and particulate materials in rock varnish appear to be detrital and atmospherically deposited (Potter and Rossman, 1977; Perry and Adams, 1978). The importance of atmospheric fluxes as supply routes for both dissolved and particulate matter to rock varnish-coated surfaces is supported by a wide variety of trace element and isotopic data (Harrington et al., 1990; Fleisher et al., 1999; Broecker and Liu, 2001; Moore et al., 2001; Bao et al., 2001; Bao and Reheis, 2003; Hodge et al., 2004).

If atmospheric chemical signatures can be preserved in rock varnish, then its trace element and isotopic signatures may preserve a record of ambient airborne components over time. Lichens and mosses have been used for decades as passive environmental indicators for trace elements, and are routinely processed for solution analysis by inductively coupled plasma mass spectrometry (Reimann et al., 2001b,c; Bargagli et al., 2002). No one has yet developed a similarly rapid and reliable technique for the sampling and analysis of <200 μm thick rock varnish coatings. Coatings and films have been sampled by scraping and selective dissolution. However, scrapings may contain considerable amounts of the rock substrate (Engel and Sharp, 1958; Reneau et al., 1991; Dragovich, 1998). Laser ablation (LA) can be used in conjunction with ICPMS to remove and rapidly analyze a ∼30 μm-thick surface layer directly from a solid substrate. Archaeologists and materials scientists have used this approach to obtain major and trace element data on human fingernails, painted and slipped pottery, and layered ceramics and composites (Kanicky et al., 1997; Mank and Mason, 1999; Speakman and Neff,

2002; Neff, 2003; Bleiner et al., 2000, 2003; Rodush-kin and Axelsson, 2003).

For this study, LA-ICPMS was used to acquire semi-quantitative major and trace element data from rock varnish samples from two locations in the southwestern United States. All data presented here represents analyses conducted using the LA microprobe in raster mode. Single spot depth-profile data were also collected, but will be presented elsewhere. This study is the first step toward developing a robust, repeatable analytical strategy for the acquisition of trace element and isotopic data from rock varnish. In addition to their potential value as a diagnostic indicator for heavy metal and radionuclide transport through the Earth's atmosphere, these data will also contribute to a deeper understanding of the processes involved in rock varnish formation.

2. Background

2.1. Rock varnish chemistry – previous work

Electron microprobe, SEM, and EDAX studies (Bauman, 1976; Douglas, 1987; Raymond et al., 1991; Reneau et al., 1992; Dragovich, 1998; McKeown and Post, 2001; Diaz, 2004) show that the typical major constituents of rock varnish include MnO, Fe_2O_3, SiO_2, Al_2O_3, CaO, MgO, K_2O, TiO_2, CO_2, and P_2O_5. Scanning electron microscope (SEM) traverses normal to varnish microlaminations show that Mn content typically correlates with Ba and Ca, and anti-correlates with Al, Si, K, Mg and Fe (Raymond et al., 1991; Reneau et al., 1992).

There is little data on the trace element chemistry of rock varnish. A comprehensive study by Engel and Sharp (1958) used a variety of techniques to discern major and trace element concentrations in 22 rock varnish samples from southern California, USA. They identified Ti, Ba and Sr as the most abundant trace elements (700–3900 ppm), with Cu, Ni, Zr, Pb, V, Co, La, Y and B present in lesser quantities (60–260 ppm) in all samples. Several elements (Cd, Ag, Nb, Sn, Ga, Mo and Be) were detected in some samples, but not in others. Tungsten was detected in one sample, but the authors attributed this to contamination (Engel and Sharp, 1958, p. 503). Recent studies (Broecker and Liu, 2001; McKeown and Post, 2001; Diaz, 2004; Thiagarajan and Lee, 2004) identify Pb, Ba, Sr, V, Ce, Zn and Zr as the most significant trace constituents in rock varnish, occurring at levels from >5000 (Pb

and Ba) to several hundred ppm. Broecker and Liu (2001), Diaz (2004) have documented extremely high Pb levels in the topmost layer of rock varnish from localities in the Southwestern USA. Fleisher et al. (1999) reported 7.5–52.7 ppm U, and 28.6–203 ppm Th in rock varnish from the Idaho Scablands.

2.2. Geologic setting

Rock varnish samples were collected from an area north of the San Juan River, near Comb Ridge in southeastern Utah, USA (Fig. 1). These samples consist of loose, rounded pebbles of porphyritic volcanic rock from the northern bank of the San Juan River, between the towns of Bluff and Mexican Hat. Varnish-coated pebbles occur in small depressions on exposed pavements of Navajo sandstone (Fig. 2). The two ovoid (~2 cm by ~6 cm, ~0.75 cm thick) pebbles analyzed for this study are entirely coated with metallic, brown-black rock varnish. The bottom surfaces of these pebbles are not reddish in color, and are free of calcite and other mineral precipitate crusts. Small areas on the bottom-facing surfaces are partly scuffed and abraded, and these areas were avoided during analysis. All other samples were selected from a large suite of rock varnish samples taken from stable, exposed, basaltic and andesitic surfaces that constitute a paleoshoreline on the flanks of the Lahontan Range (Diaz, 2004), due east of the Carson Sink, approximately 15 km SE of the town of Fallon, NV (Fig. 3).

3. Analytical methods

3.1. Electron microprobe analysis

The San Juan samples were analyzed (Table 1) using a Cameca SX100 electron microprobe (1 μm beam diameter; 30 nA beam current; 15 kV accelerating voltage) in wavelength dispersive mode, with the beam normal to the varnish layering. A JEOL 8900 JXA electron microprobe in wavelength dispersive mode (~1 μm beam diameter; 30 nA beam current; 15 kV accelerating voltage) was used to analyze rock varnish of selected samples from the Lahontan Range (Diaz, 2004). Microprobe analyses of the Lahontan samples (Table 1) are averages of numerous individual spot analyses from traverses taken at the middle of each discrete varnish lamination, roughly parallel to the layering. The relatively high standard deviations of the averaged electron
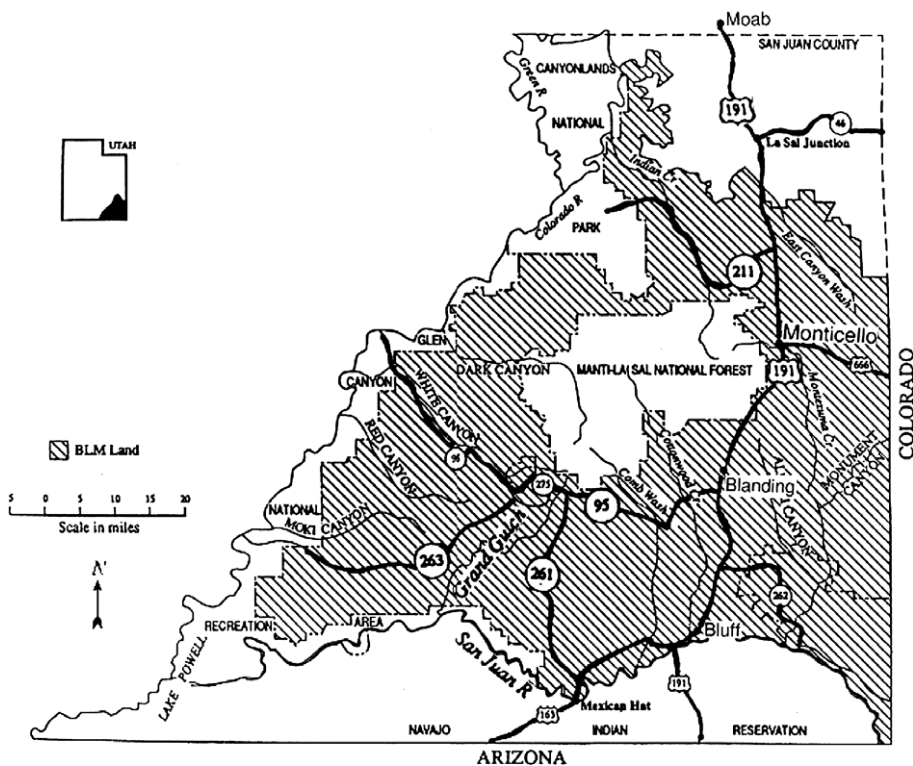
Fig. 1. Location map for the San Juan rock varnish samples. Two varnish-coated pebbles were collected from the northern bank of the San Juan River, between the towns of Bluff and Mexican Hat, in the southeastern corner of the mapped area. Map provided courtesy of the Utah Bureau of Land Management, Monticello Field Office (http://www.blm.gov/utah/monticello/index.html).

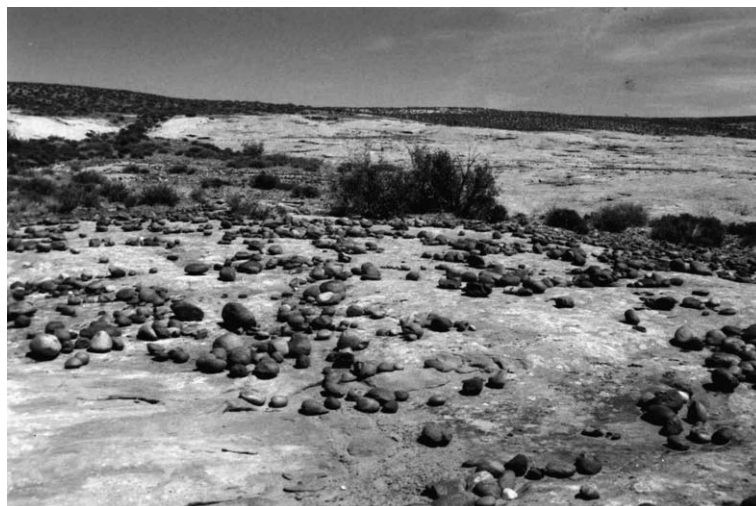Fig. 2. Sampling site for the San Juan River (UT) pebbles. Varnish-coated pebbles occur in depressions on exposed Navajo Sandstone pavement.

microprobe analyses reflect the inhomogeneous nature of rock varnish. Aluminum is the least variable major element, and was used as the internal standard for LA-ICPMS analysis.

3.2. LA-ICPMS analyses

A ThermoFinnigan-MAT 'Element 2' high resolution ICPMS, equipped with a New Wave/
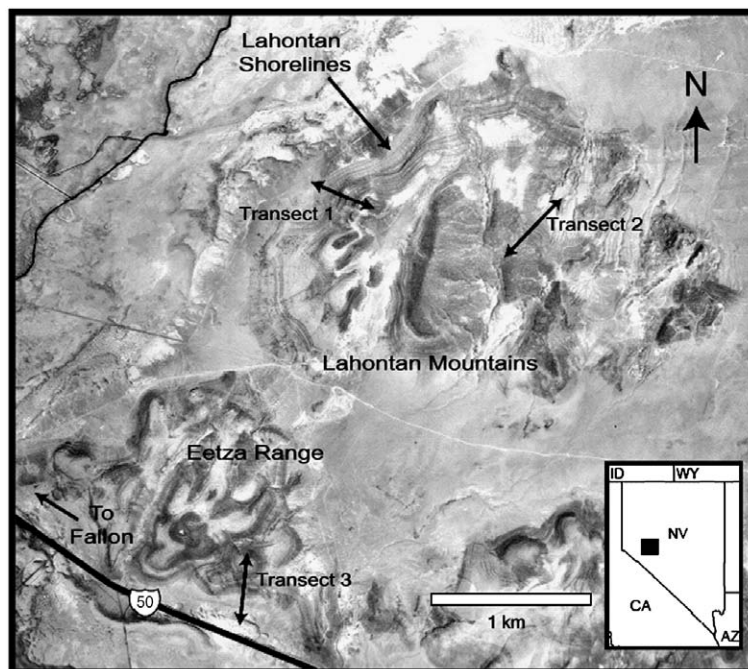
Fig. 3. Aerial photograph of the Lahontan (Churchill Co., Nevada, USA) rock varnish study area. Samples were collected along two transects; one in the Lahontan Mountains (Transect 2: Samples 12A and 13B), and one within the Eetza Range (Transect 3: Samples 15B and 17A).

Merchantek-EO 'GLUV 266X' Nd-YAG laser ablation (LA) microprobe was used to gather trace and major element data. The primary goal of LA-ICPMS analysis was to remove as much of the varnish as possible, while minimizing the concomitant removal of the rock substrate. Laser parameters and LA-ICPMS analytical settings are summarized in Table 2. Mass resolution settings for each isotope are summarized in Table 3. Prior to analysis, all samples and standards were ultrasonically cleaned in high purity water, rinsed in acetone, and dried. Individual varnish-coated rock chips were mounted in the LA chamber, which was then sealed, purged of air, and filled with Ar. Laser ablation removed the top layer of the sample as a fine powder, which was entrained in an Ar gas stream, conveyed to a Tracey spray chamber, and injected into the ICPMS ion source for ionization and mass analysis.

Data were collected with the laser in raster mode. Site selection, laser focusing, and ablation control were monitored using a video camera aimed down the laser axis, and beam diameter was estimated by measuring the diameter of the resulting crater at the sample surface (e.g., Fig. 4). Analyses were performed using a 250 μm laser at 20 Hz, and a 50 μm laser at 10 Hz. The resulting beam energies at the sample surface were 1.8 and 1.3 mJ, respectively, for a total power density of 3.67 J/cm^2 (250 μm beam) or 66.2 J/cm^2 (50 μm beam). Analytical blanks were quantified by analyzing the Ar stream from the laser ablation cell with the laser turned off, and were determined after every calibration, and after every sample change. Detection limits were less than 10 ppb for all elements, and were based on the equivalent concentration of 3X the standard deviation of the signal from 10 analyses of the gas blank, and 10 repeat analyses of NIST SRM 614.

Six glass standards (MPI-DING Reference glasses ATHO-G, GOR-132-G, StHs6-80-G, and NIST SRM-610, -612, and -614) provided calibration curves for 29 elements. All standards were pre-ablated, and a rectangular region (~2 mm^2) inside the pre-ablated area was selected for calibration analyses. Calibration curves for each element have $r^2 \geqslant 0.993$. Following the determination of calibration curves and blank subtraction, trace element data were quantified from corrected beam intensities by using the $^{27}Al^+$ signal as an internal standard. The average Al concentration for each sample was derived from the corresponding electron microprobe analysis (Table 1).

Table 1
Electron microprobe data for rock varnish samples from San Juan and the Lahontan Range (Lh12A1, Lh13B1, Lh15B1, Lh17A)

San Juan				Lh12A1				Lh13B1			
n = 11	El. wt.%	SD	%RSD	n = 12	El. wt.%	SD	%RSD	n = 7	El. wt.%	SD	%RSD
Na	0.09	0.13	143.1	Na	0.18	0.17	91.5	Na	0.51	0.62	122.6
Mg	1.73	0.25	14.7	Mg	1.30	0.28	21.9	Mg	1.18	0.28	23.7
Al	10.8	1.6	15.1	Al	8.51	0.91	10.6	Al	7.33	0.77	10.5
Si	16.5	2.0	12.0	Si	10.93	2.51	23.0	Si	10.9	1.2	11.4
P	0.24	0.11	47.0	P	n.a.			P	n.a.		
K	1.18	0.52	44.0	K	1.24	0.35	28.3	K	1.17	0.18	15.0
Ca	0.72	0.17	23.0	Ca	1.20	0.21	17.4	Ca	1.81	0.50	27.8
Ti	0.26	0.11	40.6	Ti	1.61	0.74	45.7	Ti	3.89	3.35	86.2
Mn	10.6	2.2	21.2	Mn	15.28	4.99	32.6	Mn	13.3	3.6	27.1
Fe	5.14	0.80	15.5	Fe	13.43	2.47	18.4	Fe	13.1	2.1	16.1
Ba	0.75	0.26	34.2	Ba	0.16	0.07	41.7	Ba	0.65	0.21	33.0
Total	48.0			Total	53.8			Total	53.8		

Lh15B1				Lh17A			
n = 9	El. wt.%	SD	%RSD	n = 19	El. wt.%	SD	%RSD
Na	0.14	0.05	33.4	Na	0.18	0.21	115.7
Mg	1.38	0.32	23.5	Mg	1.61	0.30	18.5
Al	7.01	1.71	24.4	Al	8.85	1.03	11.7
Si	10.3	1.5	14.6	Si	12.0	1.8	15.2
P	n.a.			P	n.a.		
K	1.07	0.21	20.0	K	1.26	0.18	14.5
Ca	1.57	0.42	27.0	Ca	1.37	0.41	30.2
Ti	6.35	5.10	80.3	Ti	2.33	0.82	35.4
Mn	14.3	5.3	36.9	Mn	12.9	4.7	36.4
Fe	12.7	5.4	42.3	Fe	11.8	2.3	19.5
Ba	0.63	0.50	79.5	Ba	0.13	0.08	58.2
Total	55.5			Total	52.6		

Each rock varnish analysis represents the average of 9 individual analyses (3 passes, 3 runs), and are derived from the material removed during a single pass of the laser over a pre-selected raster area. Data tabulated here consist of an average of 2–6 rastered areas on a single surface. Several 4–9 mm^2 rectangular areas having macroscopically continuous varnish coatings were identified on each sample. Higher magnification revealed discontinuities in rock varnish coatings in the Lahontan samples. Typically, these are resistant quartz grains that act as topographic highs on the sample surface. Thus, the LA-ICPMS analyses represent an average bulk analysis of material, mostly rock varnish coatings plus some substrate material, removed from the sampling areas.

Even where the varnish is continuous across the analyzed area, both varnish thickness and analytical depth probably vary over the ablated surfaces. Compared to the first laser pass, Mn and Pb count rates during a second laser pass were 10^2–10^3 times lower. It is likely that the laser removed most of the varnish in one pass (Fig. 4). Thus, no pre-ablation or surface cleaning was performed on the samples prior to analysis, nor were repeat analyses performed on any of the analyzed surfaces.

3.3. Analysis of the T1-G standard

An external standard, MPI-DING glass T1-G (Jochum et al., 2000), was analyzed repeatedly from September 2002 to October 2003 to monitor analytical quality. The median values of T1-G analyses show the best correspondence to certified values (Table 4). Analytical precision for the T1-G analyses was ⩽20% RSD (1σ) for elements with concentrations ⩾10 ppm (Table 4). Analytical accuracy also varies with element abundance and, with the exception of Zn, is better than 40% for elements with concentrations ⩾25 ppm. Below 25 ppm, several elements show good correspondence (Co, Ga and As), though measured concentrations may be systematically less than (Pb, Cr, Cu and Ni), or greater than (Mo) the certified or information-only

Table 2
ICPMS and Laser ablation parameters

GLUV 266X Laser ablation settings		
	Raster spacing	325 µm (150 µm)
	Beam diameter	250 µm (50 µm)
	Laser output	40–45%
	Scan speed	200 µm/s (100 µm/s)
	Repetition rate	20 Hz (10 Hz)
	Laser energy	1.8 ± 0.2 mJ (1.3 ± 0.1 mJ)
	Laser irradiance	3.67 J/cm^2 (66.2 J/cm^2)
	Pulse width	4–6 ns
Element 2 ICPMS Settings		
Gas flows and RF	Cool gas	16 L/min
	Auxiliary gas	0.9 L/min
	Sample gas	0.9 ± 0.05 L/min
	RF Power	900 ± 35 W
Lens voltages	Extraction lens	-2000 V
	Focus	-1370 ± 50 V
	X-deflection	-2.10 ± 0.25 V
	Y-deflection	8.00 ± 0.45 V
	Shape	145 ± 5 V
Other settings	Sampling time	0.01 s
	Internal standard	$^{27}Al^+$
	Lock mass	^{38}Ar

Laser parameters in parentheses refer to the calibration and re-analysis of several samples to evaluate the effect of changing laser parameters on analytical accuracy and precision.

concentrations. Several elements (Ge, Se, Ag, Sn, Sb, Au and Tl) in T1-G were at, or below, their limits of detection.

The precision and accuracy of the T1-G analyses conducted using a 50 µm diameter beam at 10 Hz were similar to those obtained using the 250 µm diameter beam at 20 Hz for most elements. Analyses using the higher laser irradiance (50 µm beam) returned higher concentrations of relatively volatile elements such as P, S, K, Cs and Ba (Table 4), though the concentrations of some refractory elements (Sc, Zr, Th and U) were also slightly higher relative to analyses conducted using a lower laser irradiance. Lower overall count rates from the 50 µm analyses resulted in decreased sensitivity for

several elements (As, Ag, W and Tl). Thus, the 250 µm beam was used for most of the subsequent analyses.

4. Rock varnish: major and trace element data

4.1. Major elements

To confirm that the varnish-bearing surfaces are, in fact, chemically distinct from weathered rock surfaces, varnish-coated and uncoated rock surfaces on one sample were analyzed (Lh12A). The varnish-coated area contains 10× to 60× higher concentrations of Mn, Co, As, Mo, Sb, Ba, W, Tl, Pb, Th and U than the weathered, unvarnished surface of the same sample (Fig. 5). By contrast, Si, Sc, Ti, V, Fe, Cr, Ga and Ag in the varnished and unvarnished regions of the same surface are equal (within analytical error), or only slightly greater in the varnished surface (Fig. 5).

A comparison of the average major element concentrations obtained using electron microprobe and LA-ICPMS (Figs. 6 and 7) reveals far less correspondence than that observed between the certified and measured values shown in Table 4 for the T1-G glass standard. Though LA-ICPMS is not an ideal technique for major element measurements, the microprobe and Al-normalized LA-ICPMS analyses of the San Juan varnish samples show considerable overlap at the 2σ level (Fig. 6), and agree to within 50% for the major and minor elements, with the exception of P and Ti. Silicon shows the best correspondence, while Mn is lower and Fe is somewhat higher in most LA-ICPMS analyses. Major element concentrations obtained using the 50 µm beam do not overlap those determined using the 250 µm beam (Fig. 6).

Conversely, microprobe and LA-ICPMS analyses of the Lahontan samples show little or no overlap at the 2σ level (Fig. 7). For a given sample, the Si content is higher, and Fe, Mn, and Ti are consistently lower, in the LA-ICPMS analyses. Analyses of the

Table 3
Analytical setup for LA-ICPMS analyses

Low resolution ($M/\Delta M = 300$)	^{9}Be, ^{27}Al, ^{35}Cl, ^{107}Ag, ^{111}Cd, ^{118}Sn, ^{121}Sb, ^{138}Ba, ^{184}W, ^{205}Tl, ^{208}Pb, ^{209}Bi, ^{232}Th, ^{238}U
Medium resolution ($M/\Delta M = 4000$)	^{27}Al, ^{28}Si, ^{31}P, ^{38}Ar, ^{45}Sc, ^{47}Ti, ^{51}V, ^{52}Cr, ^{55}Mn, ^{56}Fe, ^{59}Co, ^{60}Ni, ^{63}Cu, ^{66}Zn, ^{69}Ga, ^{93}Nb, ^{100}Mo, ^{133}Cs
High resolution ($M/\Delta M = 7000$)	^{27}Al, ^{72}Ge, ^{75}As, ^{77}Se, ^{98}Mo

Fig. 4. Photomicrograph of a rock varnish surface (SJ-CT1) following a single laser ablation pass (250 μm beam). The dark, lustrous areas between raster traces are representative of typical varnish-bearing surfaces before laser ablation.

Lahontan rock varnish samples using the 50 μm beam overlap those conducted using the 250 μm beam, and did not show the systematic differences in major element contents seen in the San Juan samples (Fig. 7). The differences between the 50 μm and 250 μm analyses are on the same order as those observed for a sample (Lh17B) that was analyzed on two different occasions using the 250 μm beam.

It is possible that an incident electron beam normal to the varnish surface produced an excitation volume similar to the volume of material removed by the incident laser beam. Thus, it may be significant that the San Juan samples were analyzed with the electron beam normal to the varnish layering, while the Lahontan rock varnish analyses were done with the beam parallel to layering. The enhancement of Si with a concomitant decrease in Mn, Fe, and Ti in the Lahontan samples also suggests that the Si-rich, Mn-poor rock substrate was co-ablated during LA-ICPMS analysis. The microprobe analyses show strong correlations between Si and K, and strong anti-correlations between Mn and Si, Ti and Si, and Ba and Si (Fig. 7). Similar trends have been observed in microprobe and SEM analyses of rock varnish from other localities (e.g., Reneau et al., 1992). However, these trends are not apparent within the LA-ICPMS data set (Fig. 7), which sug-gests that some component in the LA-ICPMS analyses may come from another source.

4.2. Trace elements

All varnish samples analyzed for this study have rich and varied trace element concentrations (Tables 5 and 6). Barium and Pb are, by far, the most abundant trace elements in all samples except for the bottom-facing surfaces of the San Juan pebbles. In these samples, Ba is the most abundant trace element, while Zr (in SJ-B1, SJ-B2) or Zn (SJ-B3) contents exceed those of Pb. At Lahontan, trace elements with concentrations in excess of 100 ppm (in order of abundance) are: Ba > Pb > Zn ≈ Co ⩾ V ⩾ As ⩾ Th ⩾ W > Cu ⩾ Ni. Elements with concentrations between 100 ppm and 10 ppm include (in order of abundance) S > Mo ⩾ Sc ≈ Nb > Cr ⩾ U ⩾ Ga > Cd. Elements typically present in concentrations below 10 ppm include Be, Se, Ag, Sn, Sb, Cs, Au, Tl and Bi. In addition to the elements listed above, appreciable trace concentrations of Zr (472 ppm in one sample) and Cl were also detected in several of the Lahontan samples (Table 5). For two Lahontan samples (13B and 15B), there were no statistically significant differences between the

Table 4
LA-ICPMS analyses of the T1G Glass Standard (Jochum et al., 2000), with a comparison of maximum, minimum and median values, and deviations from the certified values

Isotope	n	250 μm			50 μm	Certified[a]	% Deviation			
		Maximum	Minimum	Median	October 2003	(ppm)	Median	Maximum	Minimum	50 μm
[9]Be	8	5.8	1.9	2.2	5.2	*2*	12	192	−4	158
[28]Si	8	280,172	207,540	268,074	287,866	*273,000*	−2	3	−24	5
[31]P	8	866	512	729	960	*770*	−5	12	−33	25
[32]S	2			0.92	1.94	n.v.				
[35]Cl	7	144	80	119	n.a.	*90*	33	60	−11	
[39]K	2			11,248	20,803	16,100	−30			29
[45]Sc	8	25.6	22.9	25.1	31.8	26.7	−6	−4	−14	19
[47]Ti	8	5305	3945	5088	4393	4400	16	21	−10	0
[51]V	6	173	117	165	161	*190*	−13	−9	−38	−15
[52]Cr	4	14	9	11	16	22	−51	−38	−58	−29
[55]Mn	8	1148	729	984	932	1010	−3	14	−28	−8
[56]Fe	8	49,083	41,815	46,924	42,956	49,900	−6	−2	−16	−14
[59]Co	8	16.7	11.8	15.9	18.5	19	−16	−12	−38	−3
[60]Ni	4	11.6	5.7	9.0	9.7	13	−31	−11	−56	−26
[63]Cu	8	21.4	6.2	17.0	12.0	21	−19	2	−70	−43
[66]Zn	8	82.3	33.9	73.9	62.8	84	−12	−2	−60	−25
[69]Ga	8	22.1	13.8	19.9	20.2	18.6	7	19	−26	9
[75]As	7	0.93	0.63	0.77	n.d.	*0.71*	9	32	−11	
[90]Zr	2			166	233	147	13			59
[93]Nb	8	15.02	8.48	9.69	15.35	9.1	7	65	−7	69
[98]Mo	2			3.23	4.21	*5.4*	−40			−22
[100]Mo	8	8.12	6.23	7.56	10.54	*5.4*	40	50	15	95
[107]Ag	5	2.63	0.95	1.61	n.d.	n.v.				
[118]Sn	7	1.5	1.0	1.3	n.d.	2.1	−40	−31	−54	
[121]Sb	8	1.443	0.160	0.380	0.918	0.276	38	423	−42	232
[133]Cs	6	3.55	2.56	3.35	4.73	2.9	16	23	−12	63
[138]Ba	8	444	336	403	524	382	6	16	−12	37
[184]W	8	2.40	0.14	0.76	n.d.	*0.86*	−11	179	−83	
[197]Au	5	0.5	0.2	0.2	n.a.	*0.1*	103	369	102	
[205]Tl	4	0.68	0.63	0.63	n.d.	n.v.				
[208]Pb	8	8.6	2.8	6.7	7.1	13	−48	−34	−78	−45
[232]Th	8	33.0	23.4	25.4	38.5	30	−15	10	−22	28
[238]U	6	2.14	0.77	1.05	2.86	1.67	−37	28	−54	71

n.v. – no value given on certificate; n.a. – not analyzed; n.d. – not detected, or below detection limits (after blank subtraction).
All concentrations are in ppm.
[a] 'Information only' values in italics.

average trace element contents in samples analyzed using the 250 μm diameter beam, and the 50 μm diameter beam.

The trace element chemistry of rock varnish on the skyward-facing surfaces of the San Juan pebbles is distinct from that of the Lahontan Range rock varnish. After Ba and Pb, the most abundant trace elements (1000–100 ppm) in the skyward-facing surfaces of the San Juan rock varnish samples are Zn > Zr > Cu > Co > V ⩾ Ni > As. Elements with concentrations between 100 ppm and 10 ppm include (in order of abundance): Th ≈ Cd ⩾ Bi > Sc > Be > S ≈ Ga ≈ Nb ⩾ U > Mo. Elements typically present in quantities less than 10 ppm include

Se, Ag, Sb, Cs, W, and Tl. Gold, Sn and Cl were not analyzed in the San Juan samples. Chromium was analyzed, but the results consistently had errors in excess of 30% RSD, and were not considered further. Analyses conducted with increased laser irradiance on the San Juan sample returned 100% or greater concentrations (1σ) for K, Ba, Be, S, and Se and 60% or greater concentrations for Si, Pb, V, Sb, Cs, and Bi.

Several trace element concentrations are significantly different at the two localities. Rock varnish from the Lahontan Range is richer in Mo, W, Th and As than the San Juan rock varnish (Fig. 8). The skyward-facing San Juan rock varnish contains
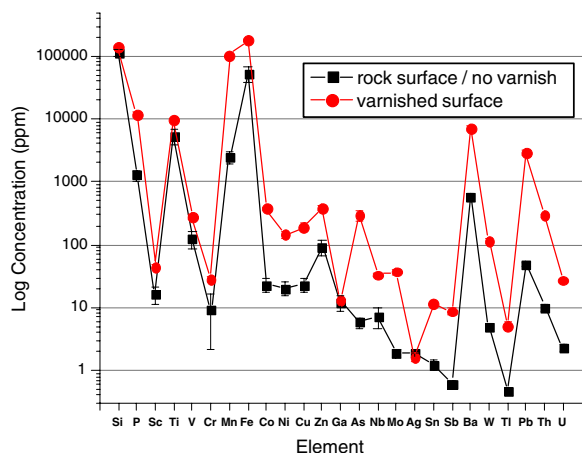
Fig. 5. Major and trace element abundances in a weathered surface lacking rock varnish (filled squares), and in rock varnish (filled circles) from the same sample (12A, Lahontan Range).

significantly higher levels of Be, Cu, Zn, Cd and Bi (Fig. 8). Differences in trace element chemistry at the two sites, and their significance, are addressed in Section 5 below.

Trace element contents also vary significantly between varnish samples taken from the skyward-facing and bottom-facing surfaces of individual varnish-coated pebbles from San Juan. If the results of the analyses performed using the 50 μm beam are not considered, average major and trace element concentrations of the bottom-facing surfaces are typically lower than those obtained from the sky-ward-facing surface of the same sample by a factor of ∼1.2 to ∼1.5. The authors speculate that the lower average trace- and major element concentrations in the bottom-facing surfaces relative to the skyward-facing surfaces may be due to lesser average varnish thickness on the bottom-facing surface. However, Pb, As, Cd, Tl and Bi concentrations from the bottom-facing varnish of the San Juan pebbles are approximately 4–9 times lower than those of the varnish on the corresponding sky-ward-facing surface of the same pebble (Fig. 8). The average concentrations of several additional elements (P, S, Cu and W) are depleted in the bot-tom-facing varnish by a factor of 2–3 relative to the skyward-facing varnish.

5. Discussion

5.1. Analytical bias in LA-ICPMS analyses

Rock varnish is, by nature, a complex and inho-mogeneous substance comprised of both chemically

precipitated and detrital solids. However, the data presented here are robust enough to suggest that some of the trends observed may be partly depen-dent on analytical methods. When compared to major element contents obtained using a non-destructive technique (electron microprobe), the results suggest that LA-ICPMS data from rock var-nish coatings may be affected by the co-ablation of substrate materials during analysis. Similar difficul-ties have also been encountered during the analysis of varnish scrapings using spectroscopic and elec-tron probe techniques (e.g., Engel and Sharp, 1958; Dragovich, 1998). Reneau et al. (1991, 1992) also found strong evidence for rock substrate involvement in non-destructive electron beam anal-yses of rock varnish. For the Lahontan samples, direct ablation of substrate was unavoidable due to the protrusion of resistant minerals through the varnish coating. If the ablatant is diluted by a rela-tively trace element-poor substrate component, then LA-ICPMS trace element data may represent mini-mum contents in rock varnish.

Analyses performed using a smaller beam diame-ter (50 μm) returned significantly higher concentra-tions for many trace and major elements in the San Juan samples. The same was true, to a lesser extent, for many of the same elements (S, K, Ba and Cs) in the T1-G glass standard (Table 4). Changing beam size made virtually no difference for analyses of rock varnish from the Lahontan Range. For the San Juan samples, the ablatant obtained using the smaller beam and slower pulse rate may simply have contained a lower percentage of substrate-derived diluent material. However, a 'purer' sampling of the varnish coating alone does not explain all of the features of the analyses per-formed using the 50 μm beam. Enhancements in some elements (K, Ba, Be, S and Se) are far greater than those seen in the other major and trace ele-ments, including those known to be vastly enriched in the rock varnish relative to the rock substrate (e.g., Mn, Pb, Co and Cd).

The power density, or irradiance, of the 50 μm laser was ∼18 times greater than that of the 250 μm diameter beam. The effects of increased laser irradiance include changes in the amount of mate-rial ablated per laser pulse, enhanced thermal effects, changes in ablatant particle size distribution, and intensification of the secondary plasma formed as the laser ionizes the carrier gas at the ablation site (Mason and Mank, 2001; Russo et al., 2002; Weis et al., 2005). Enhancements of relatively volatile ele-
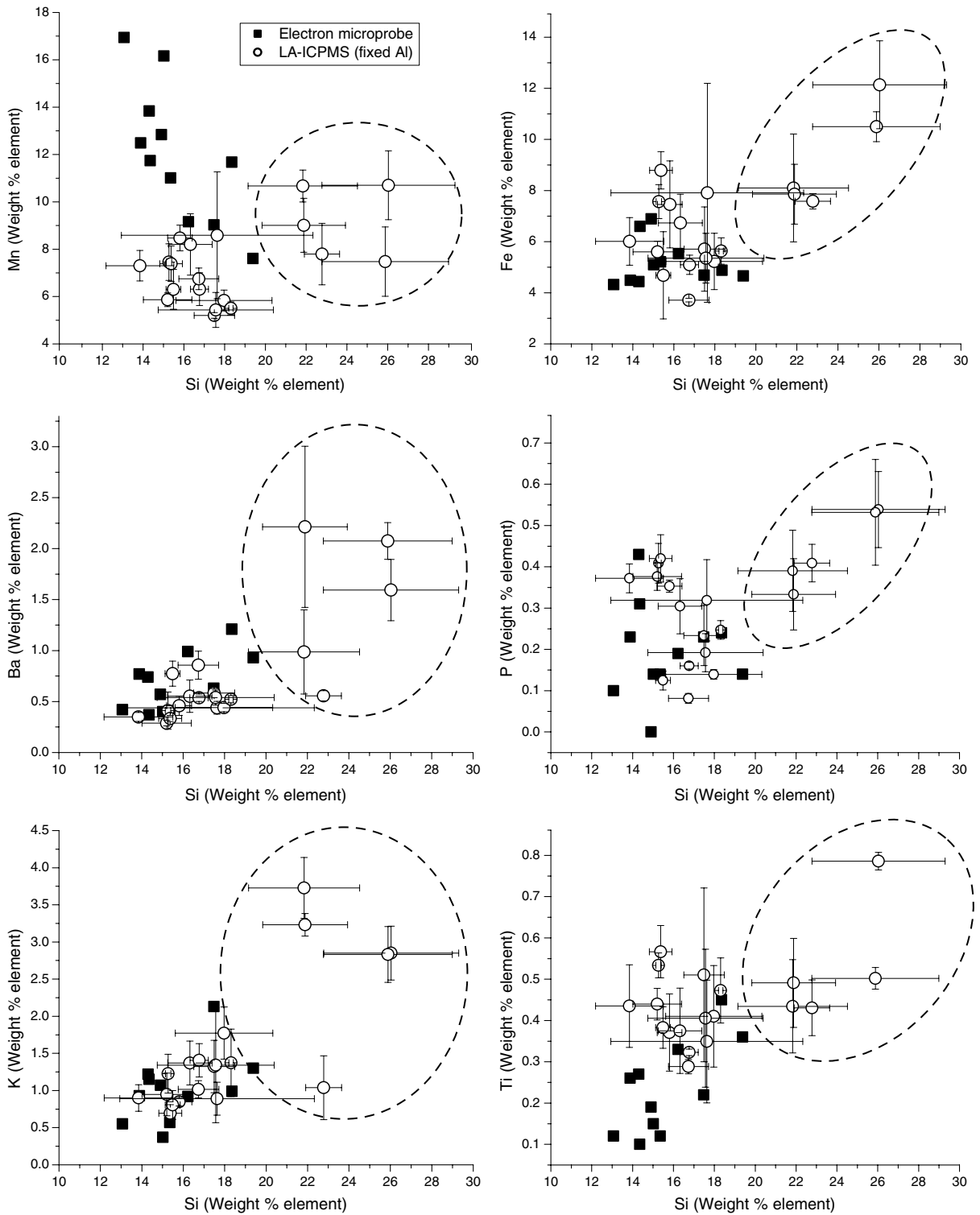
Fig. 6. Microprobe (filled squares) and LA-ICPMS (unfilled circles) analyses of Si, Mn, Fe, P, K and Ti in San Juan rock varnish. LA-ICPMS data within dashed regions were acquired using a 50 μm diameter beam. All other ICPMS data were acquired using a 250 μm diameter beam. Error bars are 2σ.
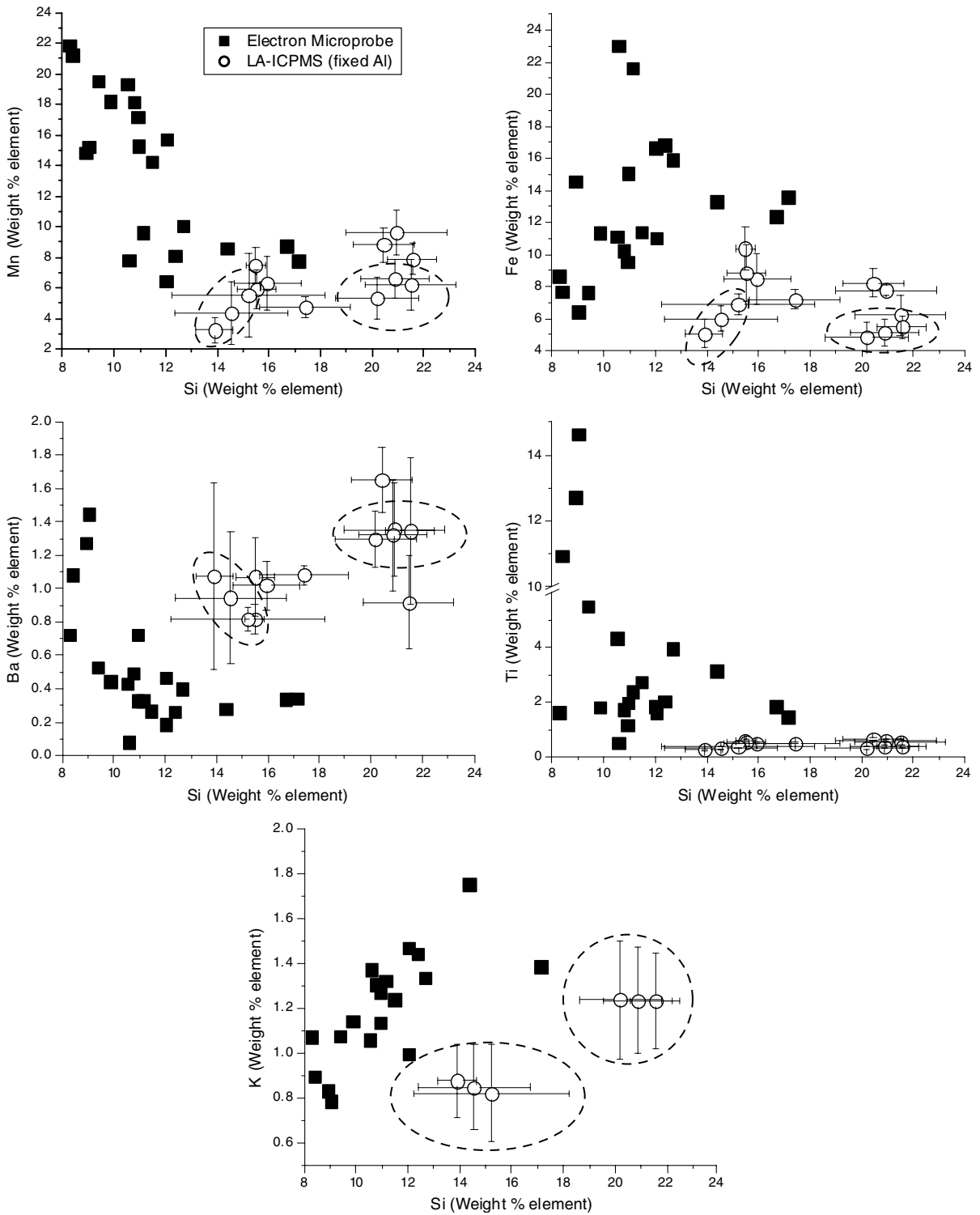
Fig. 7. Microprobe (filled squares) and LA-ICPMS (unfilled circles) analyses of Si, Mn, Fe, K and Ti in Lahontan rock varnish. LA-ICPMS data within dashed regions were acquired using a 50 μm diameter beam. All other ICPMS data were acquired using a 250 μm diameter beam. Error bars are 2σ.

Table 5
LA-ICPMS data from Lahontan Range rock varnish samples

	Lh12A-NV			Lh12A			Lh13B			Lh13B-50			Lh15B			Lh15B-50			Lh17A-1			Lh17A-2		
	El. wt.%	SD	%RSD	El. wt.%	SD	%RSD	El. wt.%	SD	%RSD	El. wt.%	SD	%RSD	El. wt.%	SD	%RSD	El. wt.%	SD	%RSD	El. wt.%	SD	%RSD	El. wt.%	SD	%RSD
Si	11.2	1.4	12.1	14.1	0.5	3.8	20.95	1.45	6.9	20.9	1.3	6.3	16.09	1.04	6.5	14.6	2.2	24.0	8.58	1.70	19.8	16.9	0.3	1.7
P	0.128	0.024	18.5	1.18	0.08	7.1	0.373	0.025	6.8	0.317	0.042	13.3	0.345	0.019	5.6	0.411	0.099	39.6	0.314	0.027	8.6	0.341	0.015	4.5
K	n.a.			n.a.			n.a.			1.23	0.24	19.3	n.a.			0.849	0.191	22.3	n.a.			n.a.		
Ti	0.533	0.148	27.8	0.989	0.059	6.0	0.596	0.068	11.4	0.358	0.054	15.0	0.525	0.060	11.4	0.319	0.060	16.7	0.538	0.072	13.4	0.409	0.040	9.7
Mn	0.250	0.055	21.9	10.2	1.2	12.2	8.22	1.24	15.0	6.59	1.22	18.6	6.10	1.15	18.8	4.38	2.05	13.4	5.78	1.21	20.9	3.48	0.47	13.4
Fe	5.27	1.41	26.7	18.1	1.0	5.5	7.40	0.78	10.5	5.13	0.85	16.5	8.73	1.26	14.4	5.98	0.80	47.7	9.63	1.68	17.5	6.67	0.58	8.7
Ba	0.058	0.008	14.1	0.706	0.075	10.6	1.31	0.22	16.8	1.32	0.33	25.1	1.00	0.13	13.4	0.945	0.399	30.1	0.700	0.184	26.3	0.557	0.070	12.6
Pb	0.0048	0.0004	8.8	0.296	0.029	9.7	0.093	0.019	20.6	0.191	0.032	17.0	0.184	0.023	12.3	0.238	0.115	49.5	0.128	0.019	14.6	0.160	0.030	18.7
	ppm			ppm			ppm			ppm			ppm			ppm			ppm			ppm		
Be	n.a.			6.3	0.3	5.3	4.89	0.64	13.2	n.a.			7.59	1.12	14.7	n.a.			6.3	0.7	11.7	2.9	0.2	6.6
S	n.a.			n.a.			n.a.			42.7	6.5	15.2	n.a.			95.5	37.8	18.8	n.a.			n.a.		
Cl	415	70	16.8	257	38	14.9	442	48	10.8	n.a.			555	61	11.1				554	49	8.9	497	67	13.5
Sc	16.0	5.0	31.6	44.7	2.2	4.9	23.4	3.1	13.2	19.0	2.9	15.3	25.5	2.8	11.0	20.0	3.8	18.9	28.8	3.5	12.1	19.5	1.6	8.4
V	126	41	32.3	274	22	7.9	248	37	14.9	159	31	19.3	234	31	13.2	156	26	33.8	308	43	13.8	151	17	11.5
Co	22.8	5.5	24.0	375	30	7.9	264	32	12.0	250	65	26.1	242	43	17.9	232	111	56.9	278	57	20.4	152	15	9.7
Ni	20.0	4.9	24.6	144	18	12.8	87.6	16.5	18.8	87.5	32.2	36.8	90.8	12.1	13.4	94.9	54.0	53.9	85.2	8.2	9.6	65.4	6.2	9.5
Cu	22.9	5.9	25.9	188	30	15.8	116	16	13.9	123	36	29.3	126	17	13.4	167	90	37.5	121	22	18.5	84.8	11.5	13.6
Zn	90.5	23.5	26.0	386	39	10.0	299	31	10.4	328	83	25.4	267	28	10.5	308	116	20.8	244	35	14.4	174	21	12.3
Ga	11.9	3.3	27.9	12.9	0.9	7.0	14.6	1.4	9.4	17.0	1.1	6.6	13.9	2.0	14.5	15.1	3.1	12.5	11.8	1.3	11.3	12.3	0.3	2.1
As	5.78	1.18	20.5	293	52	17.9	189	15	7.7	134	20	15.3	155	12	8.0	242	54	24.7	187	18	9.6	139	18	12.6
Se	n.a.			3.12	1.43	45.9	n.a.			n.a.			n.a.			n.a.			n.a.			1.57	0.56	35.9
Zr	n.a.			n.a.			n.a.			472	84	17.9	n.a.			n.a.			n.a.			n.a.		
Nb	7.11	2.57	36.2	33.1	2.8	8.3	29.2	1.5	5.0	27.2	2.0	7.4	28.8	2.4	8.5	21.6	2.7	15.6	25.3	3.5	13.8	16.5	0.5	2.9
Mo	1.90	0.29	15.3	37.1	3.6	9.6	62.0	8.4	13.6	31.9	7.9	24.7	38.0	6.0	15.9	25.5	4.0	22.5	43.2	7.0	16.2	30.0	4.4	14.8
Ag	1.92	0.02	1.2	1.62	0.24	14.8	n.a.			n.a.			1.39	0.10	7.3	n.a.			2.81	0.04	1.3	0.75	0.04	5.8
Cd	n.a.			21.7	4.5	20.9	n.a.			10.3	4.0	38.6	n.a.			20.8	13.3	26.8	n.a.			6.5	1.8	28.2
Sn	1.23	0.24	19.3	11.5	0.8	7.3	8.18	0.82	10.0	n.a.			11.2	1.0	8.9	n.a.			7.93	1.13	14.3	2.31	1.13	49.0
Sb	0.610	0.083	13.6	8.64	0.98	11.4	4.51	0.71	15.8	12.1	3.7	30.1	7.69	0.81	10.6	10.7	2.9	29.3	6.63	0.61	9.3	n.a.		
Cs				7.31	1.02	14.0	8.00	0.69	8.6	7.58	1.43	18.8	10.6	1.4	13.1	8.07	2.36	42.2	n.a.			1.77	0.83	46.7
W	4.92	0.51	10.3	112	9	8.4	244	42	17.2	147	33	22.6	148	11	7.7	121	36	55.1	101	11	11.3	71.3	13.4	18.8
Au	0.294	0.002	0.8	n.a.			0.189	0.006	3.4	n.a.			n.a.			n.a.			0.457	0.014	3.1	n.a.		
Tl	0.460	0.014	3.0	5.09	0.82	16.2	n.a.			2.47	1.05	42.6	5.96	1.31	21.9	10.7	5.9	48.5	4.22	0.91	21.5	2.91	0.98	33.6
Bi				12.6	1.0	7.8	n.a.			7.13	2.01	28.1	n.a.			9.06	4.48	36.2	n.a.			2.1	1.1	53.8
Th	10.1	1.4	13.9	290	18	6.2	113	13	11.5	107	18	16.9	172	19	10.9	115	42	38.2	129	22	17.1	115	22	19.0
U	2.30	0.30	12.8	27.1	2.7	10.1	15.2	2.9	18.9	15.6	2.5	15.7	28.6	4.4	15.2	27.8	10.6	14.9	26.7	2.9	11.0	12.9	2.9	22.8

Each column represents data from 2 to 5 separate 9-run analyses using a 250 μm beam. 'NV' denotes a non-varnished rock surface, '50' denotes analyses performed using a 50 μm beam.
n.a. – not analyzed.

Table 6
LA-ICPMS data from the San Juan rock varnish samples

	SJ-CT1			SJ-CT2			SJT-50um			SJ-B1			SJ-B2			SJC-B3		
	El. wt.%	SD	%RSD	El. wt.%	SD	%RSD	El. wt.%	SD	%RSD	El. wt.%	SD	%RSD	El. wt.%	SD	%RSD	El. wt.%	SD	%RSD
Si	18.1	2.5	13.6	14.9	1.1	7.1	23.9	2.8	11.8	17.2	0.7	3.9	17.9	2.1	11.8	16.1	0.7	4.6
P	0.346	0.064	18.5	0.394	0.045	11.3	0.449	0.103	22.9	0.188	0.045	23.9	0.193	0.030	15.8	0.103	0.018	17.7
K	1.04	0.28	27.4	0.94	0.22	23.5	3.16	0.34	10.8	1.27	0.25	19.6	1.50	0.56	37.2	0.91	0.16	17.7
Ti	0.381	0.107	28.1	0.494	0.064	13.0	0.553	0.080	14.4	0.398	0.124	31.1	0.429	0.128	29.8	0.336	0.038	11.2
Mn	8.26	1.65	19.9	7.00	0.64	9.2	9.46	1.23	13.0	5.96	0.47	7.9	5.59	0.52	9.3	6.53	0.68	10.4
Fe	7.42	2.38	32.0	6.99	0.71	10.2	9.65	1.51	15.7	5.31	1.03	19.4	5.40	0.90	16.6	4.20	1.21	28.8
Ba	0.501	0.101	20.1	0.345	0.096	27.9	1.72	0.48	27.9	0.535	0.041	7.7	0.501	0.053	10.6	0.815	0.130	16.0
Pb	0.261	0.046	17.7	0.262	0.060	23.1	0.451	0.050	11.1	0.025	0.002	6.1	0.024	0.003	11.9	0.042	0.007	16.9
	ppm			ppm			ppm			ppm			ppm			ppm		
Be	16.2	1.1	7.1	18.3	0.8	4.6	36.9	4.2	11.3	16.2	1.2	7.5	17.9	1.1	6.4	12.6	0.8	6.6
S	8.07	3.97	49.1	14.8	2.5	16.6	44.5	18.5	41.6	3.74	0.73	19.6	4.47	0.95	21.4	4.37	1.29	29.6
Sc	32.7	7.5	23.1	33.2	3.6	10.8	43.8	3.8	8.6	24.9	4.8	19.2	26.1	3.6	13.9	22.7	5.9	25.8
V	135	31	22.9	135	10	7.1	227	17	7.6	93.1	24.6	26.4	95.3	17.1	18.0	84.3	17.3	20.6
Co	219	36	16.4	231	21	9.2	301	41	13.8	178	16	8.8	180	14	7.9	164	11	7.0
Ni	111	18	16.6	144	23	15.9	160	12	7.7	80.1	9.0	11.2	79.3	8.4	10.6	107	9	8.2
Cu	289	51	17.6	338	46	13.5	383	66	17.2	57.1	8.4	14.8	70.2	24.8	35.3	315	101	32.2
Zn	550	101	18.4	538	91	16.9	762	103	13.5	200	34	16.8	224	48	21.6	596	185	31.1
Ga	16.1	2.3	14.0	19.9	2.0	10.0	25.6	2.1	8.1	15.4	1.6	10.7	15.6	1.5	9.8	16.5	2.0	11.9
As	36.4	9.6	26.4	107	18	16.6	135	22	16.3	10.0	1.7	17.4	9.79	2.49	25.5	7.05	0.82	11.7
Se	1.05	0.53	50.3	1.12	0.92	82.1	19.2	5.2	27.3	0.86	0.35	41.1	0.87	0.39	44.5	0.64	0.37	58.2
Zr	350	62	17.8	326	54	16.5	467	123	26.4	269	52	19.2	340	82	24.1	191	14	7.2
Nb	21.5	2.7	12.6	23.1	1.9	8.1	25.9	4.8	18.6	19.1	2.0	10.6	20.2	2.2	11.1	19.2	1.0	5.5
Mo	5.91	0.99	16.7	10.8	1.2	11.4	14.6	2.3	15.6	3.56	0.08	2.1	3.63	0.14	3.9	6.94	0.81	11.6
Ag	0.44	0.39	87.9	2.23	0.12	5.2	0.66	0.76	116.0	1.83	0.15	8.2	1.73	0.08	4.4	2.37	0.24	10.3
Cd	57.6	11.8	20.6	45.9	18.1	39.6	68.4	20.7	30.3	7.25	0.65	8.9	8.85	1.37	15.4	9.61	1.81	18.8
Sb	5.45	0.53	9.7	4.78	0.53	11.0	8.07	0.87	10.8	2.44	0.21	8.6	2.43	0.14	5.7	3.40	0.33	9.7
Cs	4.46	0.44	9.9	4.70	0.84	17.8	8.08	1.13	14.0	5.42	0.51	9.5	5.09	0.45	8.8	6.02	0.60	9.9
W	4.44	0.49	10.9	7.56	0.52	6.8	5.46	0.92	16.9	2.28	0.18	8.1	2.68	0.37	13.6	3.61	0.59	16.2
Tl	5.52	1.69	30.6	4.58	0.99	21.7	4.62	1.04	22.6	1.31	0.12	8.9	1.54	0.17	11.2	1.13	0.05	4.6
Bi	29.4	5.3	17.9	32.6	7.1	21.8	57.4	7.9	13.8	n.d.			n.d.			15.8	5.8	36.4
Th	42.7	4.9	11.5	52.6	5.2	9.9	64.9	17.0	26.2	30.9	5.1	16.5	32.9	4.9	14.8	26.4	1.7	6.4
U	7.08	0.87	12.2	14.2	1.8	12.7	19.4	1.5	7.8	6.09	1.80	29.6	6.79	1.38	20.4	3.62	0.48	13.2

Each column represents data from 2 to 5 separate 9-run analyses using a 250 μm beam. "T" refers to top-facing (skyward) surfaces, "B" refers to bottom-facing surfaces, '50' denotes analyses performed using a 50 μm beam.
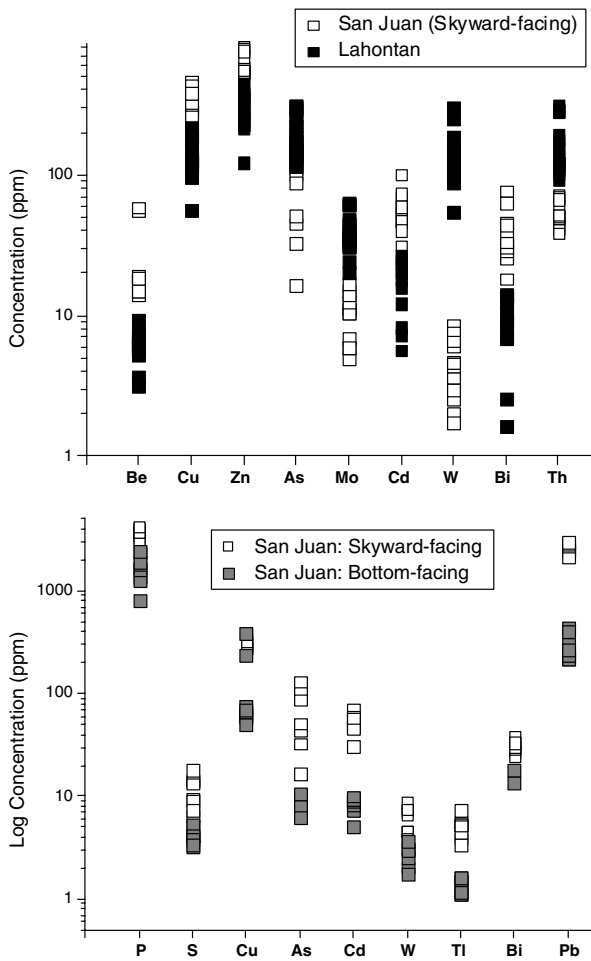n.a. – not analyzed.

Fig. 8. Trace element concentrations (Log 10 scale) in rock varnish from the Lahontan Range, NV (upper plot) and from the San Juan River area, UT (upper and lower plots). Significant differences in trace element content are apparent between the two sample sites, and on different surfaces of the same sample.

ments such as K, S, Cs, and Se with greater laser irradiance may be due to increased thermal effects, and the differing optical absorbencies of the standards and samples.

Recent studies of the effects of laser–solid interactions on LA-ICPMS data have documented a variety of processes that conspire to cause elemental fractionation leading to analytical bias (Fryer et al., 1995; Longerich et al., 1996; Eggins et al., 1998; Figg et al., 1998; Durrant, 1999; Rodushkin et al., 2002a,b; Russo et al., 2002; Guillong et al., 2003; Hattendorf et al., 2003; Weis et al., 2005). A number of these are directly applicable to the analysis of rock varnish as performed for this study.

Matrix effects, including differences in the behavior of certain elements during the ablation process (e.g., Longerich et al., 1996) may be significant, as the calibration standards used are relatively homogenous, optically translucent silicate glasses. However, the NIST SRM 61X series glass standards have been used to obtain reasonably accurate trace element analyses from a variety of oxide minerals (Gunther et al., 2000; Zack et al., 2002), and synthetic fluorite (Koch et al., 2002). The rough and uneven surfaces of the varnish samples caused noticeable beam defocusing as the sample was translated. Defocusing of the laser beam during analysis can also lead to systematic analytical errors as a result of changing ablation conditions (Ohata et al., 2002). The different light-absorbing properties of the NIST SRMs (light to dark blue glass), the MPI-DING Reference glasses (black to dark green/black) and the opaque, reflective rock varnish will result in different responses to a 266 nm laser beam of a given irradiance in Ar. Weis et al. (2005) have shown that penetration depth decreases with increasing absorbance, resulting in greater energy per volume, and smaller ablant particle size. Changing particle size distributions alter both the transport efficiency, and the degree of vaporization, atomization, and ionization of the successfully transported material in the ICP plasma (Figg et al., 1998; Guillong et al., 2003; Hattendorf et al., 2003). Thus, changes in the particle sizes available to the plasma produce analytical bias as the constituents of the most easily transported and smallest particles are preferentially vaporized, atomized, and ionized (Weis et al., 2005).

Fractionation due to ablant particle size distribution could be exacerbated when sampling a laterally and vertically heterogeneous, layered surface coating such as rock varnish. Though it is well-indurated, the cellular, porous nature of rock varnish is readily apparent in SEM and TEM images. Recent studies (Krinsley, 1998; Probst et al., 2002; Flood et al., 2003) have identified Mn-rich micro-concretions within rock varnish layers. Potter and Rossman (1977), Perry and Adams (1978), Raymond et al. (1991), Reneau et al. (1992), McKeown and Post (2001) have also identified a host of authigenic and included phases within rock varnish coatings. The presence of such micro-heterogeneities will contribute to changes in ablation efficiency and laser absorbance during analysis, which could also affect ablant particle size distribution.

5.2. Trace element contents in rock varnish

Chemical and isotopic studies (Fleisher et al., 1999; Bao et al., 2001; Broecker and Liu, 2001; Moore et al., 2001; Hodge et al., 2004; Thiagarajan and Lee, 2004) indicate that atmospherically-deposited matter plays a major role in rock varnish formation. The incorporation of atmospherically-derived material on to a surface can take place by either wet or dry deposition (Chester et al., 1997). In dry deposition, dust-sized clay- and silicate-rich eolian particulate matter is removed directly from the atmosphere by air motions, gravitational settling, or both (Wesley and Hicks, 2000). Dry particles can be entrained onto rock surfaces by minerals deposited by the evaporation of dew, rainwater, or other forms of precipitation. In wet deposition, chemical components are delivered to a surface as suspended particles, and as dissolved constituents, in rainwater, fog, snow, dew, sea spray, or river spray. The trace element contents of rainwater, fog, and other precipitation are constrained by solubility and by particle-water reactivity in clouds and precipitation, which can both be highly acidic (Chester et al., 1997). Thiagarajan and Lee (2004) propose a model whereby trace element concentrations in rock varnish are largely the result of wet atmospheric deposition, followed by trace metal scavenging.

Following wet deposition, soluble metals such as Cu and Pb may be scavenged from acidic to near-neutral solutions by the various mineral constituents of rock varnish, such as clays, amorphous silica, and Fe- and Mn-oxyhydroxides (Post, 1999; Tebo et al., 2004; Hochella et al., 2005). Scavenging by Mn- and Fe-oxyhydroxide minerals in rock varnish occurs abiotically, and would result in relatively high concentrations of heavy metals at, or very near, the surface. Preliminary depth profiling electron microprobe and LA-ICPMS analyses (Broecker and Liu, 2001; Diaz, 2004; Wayne et al., 2004) have revealed very high surface concentrations of Pb in rock varnish from several localities in the southwestern US. Broecker and Liu (2001) attribute high surface Pb concentrations in rock varnish to atmospherically-deposited automobile exhaust, though they argue in favor of a microbial mechanism for its concentration at the surface. High concentrations of Pb, or other soluble elements such as Zn, Cu, As and Co, in the topmost surface layers of rock varnish could also result from the abiotic scavenging of dissolved cations (or anions) by Fe–Mn oxyhydroxides and clays. If scavenging of dissolved elements from precipitation is an important process, their concentration profiles would probably not extend more than a few micrometers beneath the topmost surface layer, barring the development of permeable pathways that would permit solutions to come into contact with underlying varnish layers. Clearly, more analytical work must be done before this issue can be properly addressed.

Trace metals such as Co and Zn are also known to respond to the metabolic processes of Mn- and Fe-oxidizing bacteria by co-precipitating with, or sorbing preferentially onto, Fe- and Mn-oxyhydroxide biofilms in soils, fresh water, and oceanic environments (Moffett and Ho, 1996; Lienemann et al., 1997; Dong et al., 2001; Manceau et al., 2003; Nelson and Lion, 2003; Haack and Warren, 2003; Tani et al., 2003, 2004). Trace element distributions in soil Mn nodules may be intricately zoned (Palumbo et al., 2000, 2001; Liu et al., 2002; Manceau et al., 2003). Zonation may reflect temporal changes in trace element mobility and availability with changing climate, redox conditions, and soil chemistry during nodule growth. If rock varnish development is biologically mediated or catalyzed, the metabolic processes of Fe- and Mn-oxidizing bacteria and fungi may also be relevant to the development of trace element patterns within rock varnish. Trace elements such as Cu, Co and Zn may serve as necessary nutrients for microbial growth and development, or may substitute for other elements that are temporarily in short supply (Moffett and Ho, 1996; Lienemann et al., 1997). In this case, the variation of trace elements in a biogenic Fe–Mn nodule or coating may be partly dependent on microbial metabolism, population density, and growth rate, in addition to the factors listed above.

Similar trace element variations in rock varnish have not yet been observed, nor has the biogenic origin of rock varnish been established beyond reasonable doubt. However, if varnish formation is wholly or partly biogenic, it is likely that trace element concentration profiles established during varnish development would extend well beneath the topmost varnish layer. Concentration profiles could also vary systematically with the concentrations of biologically-relevant major elements such as Fe and Mn. Further applications of depth-profiling and imaging analytical techniques to the study of major and trace elemental trends in rock varnish coatings would address these questions.

5.3. Mechanisms for varying trace element signatures in rock varnish

Mosses and lichens are well established as indicators of environmental heavy metals (Garty, 1992; Getty et al., 1999; Weiss et al., 1999; Falla et al., 2000; Reimann and de Caritat, 2000; Reimann et al., 2001a,b,c; Zschau et al., 2003). Like rock varnish, the trace element chemistry of lichens and moss is highly dependent on atmospheric fluxes (Getty et al., 1999; de Caritat et al., 2001; Rizzio et al., 2001; Bargagli et al., 2002; Kirchner and Daillant, 2002; St. Clair et al., 2002; Zhang et al., 2002), and regional variations in the trace element contents of lichens and moss are attributable to nearby point sources of anthropogenic heavy metals, such as mines, smelters and coal-fired power plants (de Caritat et al., 2001; Carignan et al., 2002; Culicov et al., 2002; Ceburnis et al., 2002; Gerdol et al., 2002; Schilling and Lehman, 2002; Tsikritzis et al., 2002). The data suggest that trace element contents in rock varnish can also be interrogated to yield data that are analogous to those routinely acquired from moss and lichens. Significant regional variations in key trace elements in rock varnish are traceable to distinct and well-documented heavy metal inputs in each region.

For the San Juan samples, significant centimeter-scale variations in the contents of some, but not all, trace elements arise relative to the location of the varnish on individual pebbles. Such localized variations in trace element content may be related to the accessibility of the varnished surface to trace element-carrying agents such as rainwater or dust particles, and the ability of that surface to trap and hold the elements following deposition. The authors surmise that the markedly greater concentrations of several toxic heavy elements (Pb, Bi, Tl, Cd and As) exclusively on the skyward-facing surfaces of the varnish-coated pebbles is a response to preferential deposition of atmospherically-derived matter, either as a dissolved constituent in precipitation, or as fine particulates. This result also indicates that trace element concentrations in rock varnish may vary with the position of the varnished surface relative to the source of trace elements. For example, varnish from a vertical or inverted rock surface such as a cliff overhang may receive less atmospherically-deposited matter than varnish on a flat-lying rock outcropping nearby.

The occurrence of high levels of atmospheric Pb, Bi, Tl, Cd and As in southeastern Utah is attributable to the proximity of several large coal-fired power plants in the Four Corners region, proximal to the San Juan study area (e.g., Allis et al., 2003). During coal combustion, Pb, Tl, As, Cd, Zn and Cu are all known to be preferentially partitioned into fly ash and flue gases (Nodelman et al., 2000; Yan et al., 2001; Querol et al., 2001; Danihelka et al., 2003). Nitrogen- and S-rich stack emissions react in the atmosphere to form HNO_3 and H_2SO_4. Aqueous leaching studies show that Mo, Cd and As in coal fly ash are relatively mobile, even at ambient temperature and alkaline to near-neutral pH (Querol et al., 2000, 2001). Thus, the dissolution of labile Cd, As and other elements associated with coal fly ash particles in acidic clouds or precipitation is not completely out of the question.

The samples from the Lahontan Range are enriched in W, Mo, Th and As relative to rock varnish from the San Juan region, and from the Mojave Desert and Death Valley, eastern California (Thiagarajan and Lee, 2004). Element concentrations in these samples are derived from a variety of natural and anthropogenic sources. Large amounts of W have been dispersed into the environment in west-central Nevada, as the region lies within a major belt of W mineralization and hosts W mining and smelting sites (Diaz, 2004; Seiler et al., 2005). Tungsten and Mo are commonly associated in these ores, which are composed primarily of minerals from the scheelite–powellite (Ca(W, Mo)O$_4$) and wolframite ((Fe, Mn)WO$_4$) series. Scheelite is relatively insoluble in near-neutral aqueous solutions at 25 °C (Marinakis and Kelsall, 1987), though wolframite series minerals are soluble at 25 °C in high pH, fluoride-rich solutions derived from mine tailings (Petrunic and Al, 2005). Tungsten and As are also known to be enriched in the geothermal waters, and ground waters of the region (Seiler et al., 2005; Welch and Lico, 1988). Tungstate and molybdate ions in low pH, aqueous solutions are strongly sorbed on to Fe oxyhydroxide surfaces (Gustafsson, 2003). It is possible that the high Mo and W contents of the Lahontan rock varnish may be due a combination of dry and wet deposition, following transport from nearby mining and smelting operations.

Unlike W, As is relatively soluble and can easily be scavenged from rainwater or other precipitation by the Mn–Fe oxyhydroxide constituents similar to those found in rock varnish (Arienzo et al., 2002; Deschamps et al., 2003; Ouvrard et al., 2005). Welch and Lico (1998) attribute the high

regional As contents of shallow groundwater from the Carson Desert to the cyclic dissolution, evaporative concentration, and redeposition of elements on organic matter and Fe-oxide coatings in granite- and tephra-derived basin-fill sediments. Arsenic in these sediments could be conveyed to rock varnish by re-suspension of soil fines during high wind events, followed by dissolution and wet deposition. The high Th contents of the Lahontan Range varnish may be symptomatic of eolian particulate inputs that originate in areas dominated by granitic or rhyolitic rocks, or sediments derived there from. Although the rock varnish coats basaltic and andesitic boulders, the surrounding soils and alluvium are derived from granitic and volcanic rocks located in the Carson River Basin uplands (Lico and Seiler, 1994; Welch, 1994; Welch and Lico, 1998).

6. Conclusions

The data indicate that LA-ICPMS raster analyses of 4–9 mm^2 regions of rock varnish provide ample analytical resolution for rapid semi-quantitative determinations of both trace and major elements. The data also indicate, however, that a rock substrate component is present in most of these analyses. High-resolution LA-ICPMS permitted the detection of significant variations in trace element contents within and between the two localities included in this study. The Lahontan Range is situated within a major belt of W mineralization, and rock varnish samples from this locality contained significantly higher W and Mo contents than varnish from localities outside the W belt. Lead, Tl, Bi, Cd and As contents in the skyward-facing surfaces of varnish-coated pebbles from the Four Corners region, near the San Juan River in southeastern Utah, were an order of magnitude higher than the contents of the same elements in identical varnish from the corresponding bottom-facing surfaces. Elevated trace element content on the skyward-facing varnish surfaces indicates that these elements may be preferentially scavenged at the locations most likely to receive direct inputs of atmospherically-deposited airborne particulates. The source of metal-rich airborne particulates, in this case, is probably any one of several large coal-fired power plants in the Four Corners region, proximal to the San Juan study area. These results point to the potential utility of rock varnish as an indicator of atmospheric metal loadings.

Trace element signatures may be either cogenetic with varnish formation, or superimposed on to the varnish at a later time by wet or dry atmospheric deposition, or both. If the two processes are kinetically different, or if they result in contrasting element distribution patterns, depth profile analysis by LA-ICPMS, SIMS confocal XRF, or Auger spectroscopy may shed more light on the mechanisms by which trace elements are incorporated into rock varnish. Optimal rock varnish micro-analytical strategies would exclude or severely limit the involvement of substrate materials.

Similar studies could easily be expanded to include analyses for other components of interest, such as environmental radionuclides (e.g., Hodge et al., 2004). The data presented here further suggest that LA-ICPMS may not be the ideal analytical technique for the characterization of rock varnish trace element chemistry. The potential for entrainment of substrate materials is a particular concern, though many of the elemental fractionation issues related to particle size can be addressed fairly easily. Further work is needed to develop sampling techniques that do not inadvertently cause the co-analysis of rock substrate. Future studies could apply other direct trace analytical techniques (SIMS, XRF), or explore the possibility of dissolving the varnish directly off of the rock surface (e.g., Reneau, 1993; Neaman et al., 2004). Once these techniques are in place, 'typical' concentration ranges for a wide array of elements in rock varnish can be verified, and trends that link unusually high heavy metal concentrations to specific structures and textures within a varnish coating can be identified.

References

Al-Attar, L., Dyer, A., 2002. Sorption behaviour of uranium on birnessite, a layered manganese oxide. J. Mater. Chem. 12, 1381–1386.

Allis, R.G., Chidsey, T.C., Morgan, C., Moore, J., White, S.P., 2003. CO_2 sequestration potential beneath large power plants in the Colorado Plateau – Southern Rocky Mountain region, USA. In: Proceedings of the 2nd Annual Conference on Carbon Sequestration, Alexandria, VA, 5–8 May 2003, pp. 1–13.

Arienzo, M., Adamo, P., Chiarenzelli, J., Bianco, M.R., De Martino, A., 2002. Retention of arsenic on hydrous ferric oxides generated by electrochemical oxidation. Chemosphere 48, 1009–1018.

Bao, H.M., Reheis, M., 2003. Multiple oxygen and sulfur isotopic analyses on water-soluble sulfate in bulk atmospheric deposition from the southwestern United States. J. Geophys. Res., Atmospheres 108 (D14), ACH9-1-9.

Bao, H.M., Michalski, G.M., Thiemens, M.H., 2001. Sulfate oxygen-17 anomalies in desert varnishes. Geochim. Cosmochim. Acta 65, 2029–2036.

Bargagli, R., Monaci, F., Borghini, F., Bravi, F., Agnorelli, C., 2002. Mosses and lichens as biomonitors of trace metals. A comparison study on Hypnum cupressiforme and Parmelia caperata in a former mining district in Italy. Environ. Pollut. 116, 279–287.

Bargar, J.R., Tebo, B.M., Villinski, J.E., 2000. In situ characterization of Mn(II) oxidation by spores of the marine *Bacillus* sp. strain SG-1. Geochim. Cosmochim. Acta 64, 2775–2778.

Bauman, A.J., 1976. Desert varnish and marine ferromanganese oxide nodules – Cogeneric phenomena. Nature 259, 387–388.

Bleiner, D., Plotnikov, A., Vogt, C., Wetzig, K., Gunther, D., 2000. Depth profile analysis of various titanium based coatings on steel and tungsten carbide using laser ablation inductively coupled plasma – "time of flight" mass spectrometry. Fres. J. Anal. Chem. 368, 221–226.

Bleiner, D., Lienemann, P., Ulrich, A., Vonmont, H., Wichser, A., 2003. Spatially resolved quantitative profiling of compositionally graded perovskite layers using laser ablation-inductively coupled plasma mass spectrometry. J. Anal. Atom. Spectrom. 18, 1146–1153.

Broecker, W.S., Liu, T., 2001. Rock varnish: Recorder of desert wetness? GSA Today Aug. 2001, 4–10.

Carignan, J., Simonetti, A., Gariepy, C., 2002. Dispersal of atmospheric lead in northeastern North America as recorded by epiphytic lichens. Atmos. Environ. 36, 3759–3766.

Ceburnis, D., Sakalysa, J., Armolaitis, K., Valiulisa, D., Kvietkusa, K., 2002. In-stack emissions of heavy metals estimated by moss biomonitoring method and snow-pack analysis. Atmos. Environ. 36, 1465–1474.

Chester, R., Nimmo, M., Corcoran, P.A., 1997. Rain water-aerosol trace metal relationships at Cap Ferrat: A coastal site in the Western Mediterranean. Mar. Chem. 58, 293–312.

Culicov, O.A., Frontasyeva, M.V., Steinnes, E., Okina, O.S., Santa, Zs., Todoran, R., 2002. Atmospheric deposition of heavy metals around the lead and copper–zinc smelters in Baia Mare, Romania, studied by the moss biomonitoring technique, neutron activation analysis and flame atomic absorption spectrometry. J. Radioanal. Nucl. Chem. 254, 109–115.

Danihelka, P., Volna, Z., Jones, J.M., Williams, A., 2003. Emission of trace toxic metals during pulverized fuel combustion of Czech coals. Int. J. Energy Res. 27, 1181–1203.

de Caritat, P., Reimann, C., Bogatyrev, I., Chekushin, V., Finne, T.E., Halleraker, J.H., Kashulina, G., Niskavaara, H., Pavlov, V., Ayras, M., 2001. Regional distribution of Al, B, Ba, Ca, K, La, Mg, Mn, Na, P, Rb, Si, Sr, Th, U and Y in terrestrial moss within a 188,000 km^2 area of the central Barents region: influence of geology, seaspray and human activity. Appl. Geochem. 16, 137–159.

Deschamps, E., Ciminelli, V.S.T., Weidler, P.G., Ramos, A.Y., 2003. Arsenic sorption onto soils enriched in Mn and Fe minerals. Clays Clay Min. 51, 197–204.

Diaz, T., 2004. Investigating chemical variations in rock varnish from the Lahontan Range, Central Nevada. Unpubl. M.S. thesis, University of Nevada, Las Vegas.

Dong, D., Li, Y., Hua, X., 2001. Investigation of Fe, Mn oxides and organic material in surface coatings and Pb, Cd adsorption to surface coatings developed in different natural waters. Microchem. J. 70, 25–33.

Dorn, R.I., Oberlander, T.M., 1982. Rock varnish. Prog. Phys. Geog. 6, 317–367.

Douglas, G.R., 1987. Manganese-rich rock coatings from Iceland. Earth Surf. Proc. Landforms 12, 301–310.

Dragovich, D., 1998. Microchemistry of small desert varnish samples, western New South Wales, Australia. Earth Surf. Proc. Landforms 23, 445–453.

Durrant, S.F., 1999. Laser ablation inductively coupled plasma mass spectrometry: achievements, problems, prospects. J. Anal. Atom. Spectrom. 14, 1385–1403.

Dyer, A., Pillinger, M., Harjula, R., Amin, S., 2000. Sorption characteristics of radionuclides on synthetic birnessite-type layered manganese oxides. J. Mater. Chem. 10, 1867–1874.

Edwards, H.G.M., Moody, C.A., Jorge-Villar, S.E., Mancinelli, R., 2004. Raman spectroscopy of desert varnishes and their rock substrata. J. Raman Spectros. 35, 475–479.

Eggins, S.M., Kinsley, L.P.J., Shelley, J.M.G., 1998. Deposition and element fractionation processes during atmospheric pressure laser sampling for analysis by ICP-MS. Appl. Surf. Sci. 127–129, 278–286.

Engel, C.G., Sharp, R.S., 1958. Chemical data on desert varnish. Geol. Soc. Am. Bull. 69, 487–518.

Eppard, M., Krumbein, W.E., Koch, C., Rhiel, E., Staley, J.T., Stackebrandt, E., 1996. Morphological, physiological, and molecular characterization of actinomycetes isolated from dry soil, rocks, and monument surfaces. Arch. Microbiol. 166, 12–22.

Falla, J., Laval-Gilly, Ph., Henryon, M., Morlot, D., Ferard, J.-F., 2000. Biological air quality monitoring: A review. Environ. Monitor. Assess. 64, 627–644.

Ferris, F.G., Hallberg, R.O., Lyven, B., Pedersen, K., 2000. Retention of strontium, cesium, lead, and uranium by bacterial iron oxides from a subterranean environment. Appl. Geochem. 15, 1035–1042.

Figg, D.J., Cross, J.B., Brink, C., 1998. More investigations into elemental fractionation resulting from laser ablation-inductively coupled plasma-mass spectrometry on glass samples. Appl. Surf. Sci. 127–129, 287–291.

Fleisher, M., Liu, T., Broecker, W.S., Moore, W., 1999. A clue regarding the origin of rock varnish. Geophys. Res. Lett. 26, 103–106.

Flood, B.E., Allen, C.C., Longazo, T.G., 2003. Microbial fossils detected in desert varnish. In: Lunar and Planetary Science XXXIV, Abstr. #1633.

Fryer, B.J., Jackson, S.E., Longerich, H.P., 1995. Design, operation, and role of the laser ablation microprobe coupled with an inductively coupled plasma mass spectrometer (LAM-ICP-MS) in the earth sciences. Can. Mineral. 33, 303–312.

Garty, J., 1992. Lichens and heavy metals in the environment. In: Vernet, J.-P. (Ed.), Trace Metals in the Environment 2 – Impact of Heavy Metals on the Environment. Elsevier, Amsterdam, pp. 55–132.

Gerdol, R., Bragazza, L., Marchesinia, R., Medicia, A., Pedrinia, P., Benedetti, S., Bovolenta, A., Coppi, S., 2002. Use of moss (Tortula muralis Hedw.) for monitoring organic and inorganic air pollution in urban and rural sites in Northern Italy. Atmos. Environ. 36, 4069–4075.

Getty, S.R., Gutzler, D.S., Asmerom, Y., Shearer, C.K., Free, S.J., 1999. Chemical signals of epiphytic lichens in southwestern North America; natural versus man-made sources for airborne particulates. Atmos. Environ. 33, 5095–5104.

Guillong, M., Kuhn, H.R., Gunther, D., 2003. Application of a particle separation device to reduce inductively coupled plasma-enhanced elemental fractionation in laser ablation inductively coupled plasma-mass spectrometry. Spectrochim. Acta B 58, 211–220.

Gunther, D., Horn, I., Hattendorf, B., 2000. Recent trends and developments in laser ablation-ICP-mass spectrometry. Fres. J. Anal. Chem. 368, 4–14.

Gustafsson, J.P., 2003. Modelling molybdate and tungstate adsorption to ferrihydrite. Chem. Geol. 200, 105–115.

Haack, E.A., Warren, L.A., 2003. Biofilm hydrous manganese oxyhydroxides and metal dynamics in acid rock drainage. Environ. Sci. Technol. 37, 4138–4147.

Harrington, C.D., Reneau, S.L., Raymond Jr., R., Krier, D.J., 1990. Incorporation of volcanic ash into rock varnish, and implications for geochronologic and paleoenvironmental research. EOS Am. Geophys. Union Trans. 71, 1343.

Hattendorf, B., Latkoczy, C., Gunther, D., 2003. Laser ablation ICPMS. Anal. Chem. 75, 341A–347A.

Hochella, M.F., Moore, J.N., Putnis, C.V., Putnis, A., Kasama, T., Eberl, D.D., 2005. Direct observation of heavy metal – mineral association from the Clark Fork River Superfund Complex: Implications for metal transport and bioavailability. Geochim. Cosmochim. Acta 69, 1651–1663.

Hodge, V.F., Farmer, D.E., Diaz, T., Orndorff, R.L., 2004. Prompt detection of alpha particles from ^{210}Po: Another clue to the origin of rock varnish? J. Environ. Radioact. 78, 331–342.

Hunt, C.B., 1961. Stratigraphy of Desert Varnish. In: USGS. Prof. Pap. 424-B, Short Papers in the Geologic and Hydrologic Sciences, Articles 1–146, Geological Survey Research 1961, B194–B195.

Jochum, K.P., Dingwell, D.P., Rocholl, A., Stoll, B., Hofmann, A.W., et al., 2000. The preparation and preliminary characterization of eight geological MPI-DING reference glasses for in-situ microanalysis. Geostand. Newslett. 24, 87–133.

Kanicky, V., Novotny, I., Musil, J., Mermet, J.-M., 1997. Depth profiling of thick layers of graded metal-zirconia ceramic coatings using laser ablation inductively coupled plasma atomic emission spectrometry. Appl. Spectros. 51, 1042–1046.

Kirchner, G., Daillant, O., 2002. The potential of lichens as long-term biomonitors of natural and artificial radionuclides. Environ. Pollut. 120, 145–150.

Koch, J., Feldmann, I., Hattendorf, B., Gunther, D., Engel, U., Jakubowski, N., Bolshov, M., Niemax, K., Hergenroder, R., 2002. Trace element analysis of synthetic mono- and poly-crystalline CaF_2 by ultraviolet laser ablation inductively coupled plasma mass spectrometry at 266 and 193 nm. Spectrochim. Acta B 57, 1057–1070.

Kolb, V.M., Philip, A.I., Perry, R.S., 2004. Testing the role of silicic acid and bioorganic materials in the formation of rock coatings. In: Hoover, R.B., Levin, G.V., Rozanov, A. Yu (Eds.), Instruments, Methods, and Missions for Astrobiology VIII Proceedings of SPIE 5555, pp. 116–125.

Krinsley, D., 1998. Models of rock varnish formation constrained by high resolution transmission electron microscopy. Sedimentology 45, 711–725.

Krumbein, W.E., Jens, K., 1981. Biogenic rock varnishes of the Negev Desert (Israel): an ecological study of iron and manganese transformation by cyanobacteria and fungi. Oecologia 50, 25–38.

Kuhlman, K.R., Allenbach, L.B., Ball, C.L., Fusco, W.G., LaDuc, M.T., Kuhlman, G.M., Anderson, R.C., Stuecker, C.T., Erickson, I.T., Benardini, J., Crawford, R.L., 2005. Enumeration, isolation, and characterization of ultraviolet (UV-C) resistant bacteria from rock varnish in the Whipple Mountains, California. Icarus 174, 585–595.

Lee, M.R., Bland, P.A., 2003. Dating climatic change in hot deserts using desert varnish on meteorite finds. Earth Planet. Sci. Lett. 206, 187–198.

Lico, M.S., Seiler, R.L., 1994. Ground-water quality and geochemistry, Carson Desert, western Nevada. US Geol. Surv. Open-File Rep., pp. 94–131.

Lienemann, C-.P., Taillefert, M., Perret, D., Gaillard, J-.F., 1997. Association of cobalt and manganese in aquatic systems: Chemical and microscopic evidence. Geochim. Cosmochim. Acta 61, 1437–1446.

Liu, T.H., Broecker, W.S., 2000. How fast does rock varnish grow? Geology 28, 183–186.

Liu, T., Broecker, W.S., Bell, J.W., Mandeville, C.W., 2000. Terminal Pleistocene wet event recorded in rock varnish from Las Vegas Valley, southern Nevada. Palaeogeog., Palaeoclim., Palaeoecol. 161, 423–433.

Liu, F., Colombo, C., Adams, P., He, J.Z., Violante, A., 2002. Trace elements in manganese–iron nodules from a Chinese alfisol. Soil Soc. Am. J. 66, 661–670.

Longerich, H.P., Gunther, D., Jackson, S.E., 1996. Elemental fractionation in laser ablation inductively coupled plasma mass spectrometry. Fres. J. Anal. Chem. 355, 538–542.

Manceau, A., Tamura, N., Celestre, R.S., MacDowell, A.A., Geoffroy, N., Sposito, G., Padmore, H.A., 2003. Molecular-scale speciation of Zn and Ni in soil ferromanganese nodules from loess soils of the Mississippi Basin. Environ. Sci. Technol. 37, 75–80.

Mank, A.J.G., Mason, P.R.D., 1999. A critical assessment of laser ablation ICP-MS as an analytical tool for depth analysis in silica-based glass samples. J. Anal. Atom. Spectrom. 14, 1143–1153.

Marinakis, K.I., Kelsall, G.H., 1987. The surface chemical properties of scheelite ($CaWO_4$); I. The Scheelite/Water Interface and $CaWO_4$ solubility. Coll. Surf. 25, 369–385.

Mason, P.R.D., Mank, A.J.G., 2001. Depth-resolved analysis in multi-layered glass and metal materials using laser ablation inductively coupled plasma mass spectrometry (LA-ICP-MS). J. Anal. Atom. Spectrom. 16, 1381–1388.

McKeown, D.A., Post, J.E., 2001. Characterization of manganese oxide mineralogy in rock varnish and dendrites using X-ray absorption spectroscopy. Am. Mineral. 86, 701–713.

Misaelides, P., Katranas, T., Godelitsas, A., Klewe-Nebenius, H., Anousis, I., 2002. The chemical behavior of the natural microporous manganese oxide todorokite in actinide (Th, U, Pa) aqueous solutions. Separat. Sci. Technol. 37, 1109–1121.

Moffett, J.W., Ho, J., 1996. Oxidation of cobalt and manganese in seawater via a common microbially catalyzed pathway. Geochim. Cosmochim. Acta 60, 3415–3424.

Moore, W.S., Liu, T.Z., Broecker, W.S., Finkel, R.C., Wright, A., 2001. Factors influencing Be-7 accumulation on rock varnish. Geophys. Res. Lett. 28, 4475–4478.

Nagy, L.A., Rigali, M.J., Jones, W.D., Krinsley, D.H., Sinclair, N.A., 1991. Rock varnish in the Sonoran Desert: Microbiologically mediated accumulation of manganiferous sediments. Sedimentology 38, 1153–1171.

Neaman, A., Mouele, F., Trolard, F., Bourrie, G., 2004. Improved methods for selective dissolution of Mn oxides: Applications for studying trace element associations. Appl. Geochem. 19, 973–979.

Neff, H., 2003. Analysis of Mesoamerican plumbate pottery surfaces by laser ablation-inductively coupled plasma-mass spectrometry (LA-ICP-MS). J. Archaeolog. Sci. 30, 21–35.

Nelson, Y.M., Lion, L.W., 2003. Formation of biogenic manganese oxides and their influence on the scavenging of toxic trace metals. In: Selim, H.M., Kingerly, W.L. (Eds.), Geochemical and Hydrological Reactivity of Heavy Metals in Soils. Lewis, CRC Press, Boca Raton, FL, pp. 169–186.

Nodelman, I.G., Pisupati, S.V., Falcone Miller, S., Scaroni, A.W., 2000. Partitioning behavior of trace elements during pilot-scale combustion of pulverized coal and coal–water slurry fuel. J. Hazard. Mater. 74, 47–59.

Ohata, M., Iwasaki, Y., Furuta, N., Brenner, I.B., 2002. Studies on laser defocusing effects on laser ablation inductively coupled plasma-atomic emission spectrometry using emission signals from laser-induced plasma. Spectrochim. Acta B 57, 1713–1725.

Ouvrard, S., de Donato, P., Simonnot, M.O., Begin, S., Ghanbaja, J., Alnot, M., Duval, Y.B., Lhote, F., Barres, O., Sardin, M., 2005. Natural manganese oxide: Combined analytical approach for solid characterization and arsenic retention. Geochim. Cosmochim. Acta 69, 2715–2724.

Palumbo, B., Angelone, M., Bellanca, A., Dazzi, C., Hauser, S., Neri, R., Wilson, J., 2000. Influence of inheritance and pedogenesis on heavy metal distribution in soils of Sicily, Italy. Geoderma 95, 247–266.

Palumbo, B., Bellanca, A., Neri, R., Roe, M.J., 2001. Trace metal partitioning in Fe–Mn nodules from Sicilian soils, Italy. Chem. Geol. 173, 257–269.

Perry, R.S., Adams, J., 1978. Desert varnish: Evidence of cyclic deposition of manganese. Nature 276, 489–491.

Perry, R.S., Kolb, V.M., 2004. Biological and organic constituents of desert varnish: review and new hypotheses. In: Hoover, R.B., Rozanov, A. Yu. (Eds.), Instruments, Methods, and Missions for Astrobiology VII, Proceedings of SPIE 5163, pp. 202–217.

Perry, R.S., Dodsworth, J., Staley, J.T., Gillespie, A., 2002. Molecular analyses of microbial communities in rock coatings and soils from Death Valley California. Astrobiology 2, 539.

Petrunic, B.M., Al, T.A., 2005. Mineral/water interactions in tailings from a tungsten mine, Mount Pleasant, New Brunswick. Geochim. Cosmochim. Acta 69, 2469–2483.

Post, J.E., 1999. Manganese oxide minerals: Crystal structures and economic and environmental significance. Proc. Natl. Acad. Sci. USA 96, 3447–3454.

Potter, R.M., Rossman, G.R., 1977. Desert varnish: The importance of clay minerals. Science 196, 1446–1448.

Probst, L.W., Allen, C.C., Thomas-Keprta, K.L., Clemett, S.J., Longazo, T.G., Nelman-Gonzalez, M.A., Sams, C., 2002. Desert varnish – Preservation of biofabrics and implications for Mars. In: Lunar and Planetary Science XXXIII, Abstr. #1764.

Querol, X., Umana, J.C., Alastuey, A., Bertrana, C., Lopez-Soler, A., Plana, F., 2000. Extraction of water-soluble impurities from fly ash. Energy Sources 22, 733–750.

Querol, X., Umana, J.C., Alastuey, A., Ayora, C., Lopez-Soler, A., Plana, F., 2001. Extraction of soluble major and trace elements from fly ash in open and closed leaching systems. Fuel 80, 801–813.

Raymond Jr., R., Reneau, S.L., Harrington, C.D., 1991. Elemental relationships in rock varnish as seen with scanning electron microscopy and energy dispersive X-ray elemental line profiling. Scann. Microsc. 5, 37–46.

Reimann, C., de Caritat, P., 2000. Intrinsic flaws of element enrichment factors (EFs) in environmental geochemistry. Environ. Sci. Technol. 34, 5084–5091.

Reimann, C., Kalushina, G., de Caritat, P., Niskavaara, H., 2001a. Multi-element, multi-medium regional geochemistry in the European arctic: element concentration, variation, and correlation. Appl. Geochem. 16, 759–780.

Reimann, C., Koller, F., Frengstad, B., Kashulina, G., Niskavaara, H., Englmaier, P., 2001b. Comparison of the element composition in several plant species and their substrate from a 1,500,000-km^2 area in Northern Europe. Sci. Total Environ. 278, 87–112.

Reimann, C., Niskavaara, H., Kashulina, G., Filzmoser, P., Boyd, R., Volden, T., Tomilina, O., Bogatyrev, I., 2001c. Critical remarks on the use of terrestrial moss (*Hylocomium splendens* and *Pleurozium schreberi*) for monitoring of airborne pollution. Environ. Pollut. 113, 41–57.

Reneau, S.L., 1993. Manganese accumulation in rock varnish on a desert piedmont, Mojave Desert, California, and application to evaluating varnish development. Quat. Res. 40, 309–317.

Reneau, S.L., Hagan, R.C., Harrington, C.D., Raymond Jr., R., 1991. Scanning electron microscopic analysis of rock varnish chemistry for cation-ratio dating: An examination of electron beam penetration depths. Scann. Microsc. 5, 47–54.

Reneau, S.L., Raymond, R., Harrington, C., 1992. Elemental relationships in rock varnish stratigraphic layers, Cima volcanic field, California: Implications for varnish development and the interpretation of varnish chemistry. Am. J. Sci. 292, 684–723.

Rizzio, E., Bergamaschi, L., Valcuvia, M.G., Profumo, A., Gallorini, M., 2001. Trace element determination in lichens and in the airborne particulate matter for the evaluation of the atmospheric pollution in a region of northern Italy. Environ. Int. 26, 543–549.

Rodushkin, I., Axelsson, M.D., 2003. Application of double focusing sector field ICP-MS for multielemental characterization of human hair and nails. Part III. Direct analysis by laser ablation. Sci. Total Environ. 305, 23–39.

Rodushkin, I., Axelsson, M.D., Malinovsky, D., Baxter, D.C., 2002a. Analyte- and matrix-dependent chemical response variations in laser ablation inductively coupled plasma mass spectrometry Part 1: The roles of plasma and ion sampling conditions. J. Anal. Atom. Spectrom. 17, 1223–1230.

Rodushkin, I., Axelsson, M.D., Malinovsky, D., Baxter, D.C., 2002b. Analyte- and matrix-dependent chemical response variations in laser ablation inductively coupled plasma mass spectrometry Part 2: Implications for multi-element analyses. J. Anal. Atom. Spectrom. 17, 1231–1239.

Russo, R.E., Mao, X., Liu, H., Gonzalez, J., Mao, S.S., 2002. Laser ablation in analytical chemistry – a review. Talanta 57, 425–451.

Schilling, J.S., Lehman, M.E., 2002. Bioindication of atmospheric heavy metal deposition in the Southeastern US using the moss *Thuidium delicatulum*. Atmos. Environ. 36, 1611–1618.

Seiler, R.L., Stollenwerk, K.G., Garbarino, J.R., 2005. Factors controlling tungsten concentrations in ground water, Carson Desert, Nevada. Appl. Geochem. 20, 423–441.

Speakman, R.J., Neff, H., 2002. Evaluation of painted pottery from the Mesa Verde region using laser ablation-inductively coupled plasma-mass spectrometry (LA-ICP-MS). Am. Antiquity 67, 137–144.

Spilde, M.N., Boston, P.J., Northup, D.E., 2002. Subterranean manganese deposits in caves: Analogies to rock varnish. In: Geol. Soc. Am. Abstr. with Prog, Paper No. 216-13.

St. Clair, S.B., St. Clair, L.L., Weber, D.J., Mangelson, N.F., Eggett, D.L., 2002. Element accumulation patterns in foliose and fruticose lichens from rock and bark substrates in Arizona. The Bryologist 105, 415–421.

Tani, Y., Miyata, N., Iwahori, K., Soma, M., Tokuda, S., Seyama, H., Theng, B.K.G., 2003. Biogeochemistry of manganese oxide coatings on pebble surfaces in the Kikukawa River System, Shizuoka, Japan. Appl. Geochem. 18, 1541–1554.

Tani, Y., Ohashi, M., Miyata, N., Seyama, H., Iwahori, K., Soma, M., 2004. Sorption of Co(II), Ni(II), and Zn(II) on biogenic manganese oxides produced by a Mn-oxidizing fungus, strain KR21-2. J. Env. Sci. Health – Part A, Toxic/Hazard. Subst. & Environ. Engin. A 39, 2641–2660.

Taylor-George, S., Palmer, F.E., Staley, J.T., Borns, D.J., Curtiss, B., Adams, J.B., 1983. Fungi and bacteria involved in desert varnish formation. Microbial Ecol. 9, 227–245.

Tebo, B.M., Bargar, J.R., Clement, B.G., Dick, G.J., Murray, K.J., Parker, D., Verity, R., Webb, S.M., 2004. Biogenic

manganese oxides: Properties and mechanisms of formation. Ann. Rev. Earth Planet. Sci. 32, 287–328.

Thiagarajan, N., Lee, C.-T. A., 2004. Trace element evidence for the origin of desert varnish by direct aqueous atmospheric deposition. Earth Planet. Sci. Lett. 224, 131–141.

Tsikritzis, L.I., Ganatsios, S.S., Duliu, O.G., Sawidis, T.D., 2002. Heavy metals distribution in some lichens, mosses, and trees in the vicinity of lignite power plants from West Macedonia, Greece. J. Trace Microprobe Tech. 20, 395–413.

Wayne, D.M., Diaz, T.A., Orndorff, R.L., 2004. Atmospheric inputs of heavy metals and lead isotopes to rock varnish revealed by high-resolution laser ablation inductively coupled plasma mass spectrometry. In: Abstract of Papers of the 227th ACS National Meeting; March 28 to April 1, 2004; Anaheim, CA, American Chemical Society, 227, Pt. 2,U93.

Weiss, D., Shotyk, W., Kramers, J.D., Gloor, M., 1999. Sphagnum mosses as archives of recent and past atmospheric lead deposition in Switzerland. Atmos. Environ. 33, 3751–3763.

Weis, P., Beck, H.P., Gunther, D., 2005. Characterizing ablation and aerosol generation during elemental fractionation on absorption modified lithium tetraborate glasses using LA-ICP-MS. Anal. Bioanal. Chem. 381, 212–224.

Welch, A.H., 1994. Ground-water quality and geochemistry in Carson and Eagle Valleys, western Nevada and eastern California. US Geol. Surv. Open – File Rep. pp. 93–133.

Welch, A.H., Lico, M.S., 1988. Arsenic in an alluvial – lacustrine aquifer, Carson Desert, western Nevada. In: Ragone S.E., (Ed.), US Geological Survey Program on Toxic Water – Groundwater Contamination, October 1985, Proceedings of the US Geological Survey Open – File Rep. 86-481, E13–E18.

Welch, A.H., Lico, M.S., 1998. Factors controlling As and U in shallow ground water, southern Carson Desert, Nevada. Appl. Geochem. 13, 521–539.

Wesley, M.L., Hicks, B.B., 2000. A review of the current status of knowledge on dry deposition. Atmos. Environ. 34, 2261–2282.

Yan, R., Gauthier, D., Flamant, G., 2001. Volatility and chemistry of trace elements in a coal combustor. Fuel 80, 2217–2226.

Zack, T., Kronz, A., Foley, S.F., Rivers, T., 2002. Trace element abundances in rutiles from eclogites and associated garnet mica schists. Chem. Geol. 184, 97–122.

Zhang, Zh.H., Chai, Z.F., Mao, X.Y., Chen, J.B., 2002. Biomonitoring trace element atmospheric deposition using lichens in China. Environ. Pollut. 120, 157–161.

Zschau, T., Getty, S.J., Gries, C., Asmerom, Y., Zambrano, A., Nash III, T.H., 2003. Historical and current atmospheric deposition to the epilithic lichen Xanthoparmelia in Maricopa County, Arizona. Environ. Pollut. 125, 21–30.